Discrete and Continuous Dynamical Systems - Series S

doi:10.3934/dcdss.2024151

HIV INFECTION DYNAMICS WITH BROADLY NEUTRALIZING ANTIBODIES AND CTL IMMUNE RESPONSE

Ting Guo[1], Qi Deng[2], Shasha Gao[3], Zhipeng Qiu[4] and Libin Rong[*5]

[1]Aliyun School of Big Data, Changzhou University, Changzhou 213164, China

[2]Laboratory for Industrial and Applied Mathematics, Department of Mathematics and Statistics, York University, Toronto, ON M3J1P0, Canada

[3]School of Mathematics and Statistics, Jiangxi Normal University, Nanchang 330000, China

[4]School of Mathematics and Statistics, Nanjing University of Science and Technology, Nanjing 210094, China

[5]Department of Mathematics, University of Florida, Gainesville, FL 32611, USA

Abstract. HIV infection remains a significant global public health concern. Although current antiretroviral therapies and broadly neutralizing antibodies (bNAbs) can decrease plasma viral load, they are unable to completely eradicate the virus. Alongside these treatments, the cytotoxic T lymphocyte (CTL) immune response also contributes to viral control. However, the impact of antiretroviral drugs and bNAb therapies on HIV dynamics in the presence of CTL immune responses remains uncertain. In this paper, we develop and analyze a mathematical model that incorporates CTL immune response, bNAb, and drug therapies. We demonstrate that the basic reproduction number $\mathcal{R}_0$ and the CTL immune response reproduction number $\mathcal{R}_c$ determine the existence and stability of the equilibria. Numerical investigation reveals that both antiretroviral drugs and bNAb therapies can reduce the viral load to below the detection limit. However, bNAb therapy can delay the time to viral rebound compared with antiretroviral therapy alone. Furthermore, bNAbs have a more significant impact on viral reduction than the CTL immune response. The CTL immune response increases the number of uninfected cells and reduces the number of infected cells and viral load. Analysis of the relative contributions shows that bNAb therapy can enhance the CTL immune response, similar to the direct stimulation of antigens. These findings suggest that bNAb therapy, combined with CTL immune response, plays a critical role in HIV control and has important implications for understanding HIV pathogenesis and developing more effective treatment strategies to manage or even eliminate the disease.

1. **Introduction.** The human immunodeficiency virus (HIV) is the causative agent of acquired immunodeficiency syndrome (AIDS) and primarily targets the body's immune system, specifically CD4+ T cells. The infection of these cells increases individuals' vulnerability to opportunistic infections, cancers, and even death [26]. According to the World Health Organization (WHO), an estimated 39.0 million

2020 *Mathematics Subject Classification.* Primary: 34D20, 37N25; Secondary: 92B05.

Key words and phrases. HIV, mathematical models, broadly neutralizing antibody, CTL immune response, viral rebound.

*Corresponding author: Libin Rong.

[33.1–45.7 million] people were living with HIV at the end of 2022 [47], underscoring the ongoing global public health challenge posed by HIV infection.

Shortly after primary infection, HIV establishes a pool of infected cells containing replication-competent provirus, known as the latent reservoir. These cells can persist for an extended period and produce infectious virus particles upon activation by various stimuli [42]. Latently infected cells are considered a major obstacle to achieving HIV remission due to their insensitivity to drugs and the host immune response [21].

Current combination antiretroviral therapy (cART), which comprises a range of inhibitors targeting viral enzymes (reverse transcriptase, integrase, and protease, etc), has dramatically reduced the morbidity and mortality of HIV-infected individuals [20]. cART can suppress viral replication below the detection limit of standard clinical assays but fails to cure HIV infection because the virus rebounds when cART is discontinued [1, 26]. Consequently, individuals living with HIV require lifelong drug administration. This may lead to drug resistance, inflammation, and other non-AIDS-associated comorbidities [8]. Therefore, alternative strategies in HIV therapy that avoid drug resistance, achieve durable viral suppression, and reduce the viral reservoir are highly desirable.

The bNAb therapy offer a novel intervention for controlling HIV. They can neutralize the majority of circulating viral strains and block the infection of target cells by targeting the HIV envelope spike [7, 40, 41]. Furthermore, experiments indicate that bNAbs also increase infected cell death and accelerate the clearance of free virions [19, 24, 25]. Nishimura et al. [34] found that early bNAb therapy alone may induce sustained viral remission in simian-human immunodeficiency virus (SHIV)-infected rhesus macaques, eliminating the need for lifelong cART. Studies in animal and human models have demonstrated that bNAbs can decrease the level of cell-associated viral DNA, reflecting a reduction in the viral reservoir [6, 14, 15]. In addition to the aforementioned functions, bNAbs promote effector stimulation by enhancing antigen presentation, akin to the "vaccinal effect" observed in tumors [13]. Indeed, enhanced CTL activity has been observed in non-human primates and HIV-infected patients treated with combined bNAbs (3BNC117 and 10-1074) [32, 33]. In a clinical study [38], researchers found that individuals receiving the antibody 3BNC117 at the onset of ART initiation maintained a robust CTL immune response for up to one year.

Numerous mathematical models have been employed to enhance our understanding of HIV infection under bNAb therapy [11, 12, 48]. In their study [12], Desikan et al. fitted a mathematical model to viral load data from macaques [34] and demonstrated that short-term bNAb therapy reduces viremia and limits immune exhaustion. Yan and Wang [48] proposed a mathematical model to simulate the "shock-kill" strategy, incorporating bNAbs and HIV latency activators. They described the effect of bNAbs by modifying the infection rate of viruses and the death rates of productively infected cells and viruses. Building on the vectored immunoprophylaxis (VIP) experiment, which can elicit bNAbs [5], recent modeling approaches have shown that the "shock and kill" strategy with VIP can effectively control HIV infection [11]. However, most models neglect the direct effects of the CTL immune response in bNAb therapy. In this study, we extend the mathematical model proposed by Deng et al. [11] to include the CTL immune response. We investigate how bNAbs and ART affect the dynamics of HIV infection under the CTL immune response, elucidate the mechanisms of viral reduction, and evaluate the relative

contributions to the CTL immune response from other antigens and the activation of bNAbs.

2. Model formulation.

2.1. Model.

We develop a model of viral dynamics that includes the CTL immune response, bNAbs, and antiretroviral drug therapies. The model is described by the following system and the schematic diagram is shown in Fig. 1.

$$\begin{cases} \dfrac{\mathrm{d}H(t)}{\mathrm{d}t} = \lambda - d_1 H - \beta(1-\varepsilon)HV, \\ \dfrac{\mathrm{d}L(t)}{\mathrm{d}t} = f(1-\varepsilon)\beta HV + bL - aL - d_2 L, \\ \dfrac{\mathrm{d}I(t)}{\mathrm{d}t} = (1-f)(1-\varepsilon)\beta HV + aL - d_3 I - pZI, \\ \dfrac{\mathrm{d}V(t)}{\mathrm{d}t} = Nd_3 I - d_4 V - mAV, \\ \dfrac{\mathrm{d}A(t)}{\mathrm{d}t} = r + qAV - d_5 A, \\ \dfrac{\mathrm{d}Z(t)}{\mathrm{d}t} = (c_0 + \dfrac{c_1 A}{c_2 + A})ZI - d_6 Z, \end{cases} \tag{1}$$

where the state variables H, L, I, V, A, Z represent the concentrations of uninfected CD4+ T cells, latently infected CD4+ T cells, productively infected CD4+ T cells, free virions, bNAbs, and CTLs at time t, respectively. Uninfected CD4+ T cells are produced at a rate of λ, undergo natural death at a per capita rate of d_1, and become infected by virions at a rate of β. A fraction f of infections of uninfected CD4+ T cells results in latently infected cells, while the remainder $(1-f)$ leads to productively infected cells. Latently infected CD4+ T cells proliferate, become activated, and die at rates of b, a, and d_2, respectively. Infected CD4+ T cells die at a rate of d_3 due to viral cytopathicity and are killed by CTL immune response at a rate of p. The constant N denotes the total number of virions produced by one productively infected CD4+ T cell over its lifespan. Free virions are cleared at a rate of d_4 and are neutralized by bNAbs with a second-order rate constant of m. The constant ε represents the overall effectiveness of antiretroviral therapy in blocking cell-free virus infection of CD4+ T cells [36].

Balazs et al. [5] employed a specialized adeno-associated virus vector approach known as VIP. This method induces lifelong expression of human antibodies at super-prophylactic levels from a single intramuscular injection. Their study demonstrated that bNAbs expressed by VIP can effectively protect animals from HIV infection, even when challenged by intravenous injection with replication-competent virus at very high doses. Thus, we assume that bNAbs have a constant production rate r. Additionally, free virions stimulate the proliferation of bNAbs. Therefore, we let bNAbs proliferate at a rate of q, while d_5 represents the natural clearance rate of bNAbs.

Activation of CTLs can be facilitated not only by infected cells but also by bNAbs [13, 32, 33]. Therefore, we assume that the natural proliferation rate of CTLs is c_0. Similar to the "vaccinal effect" observed in tumors [13], bNAbs (A) trigger the proliferation of CTLs (Z). To prevent CTLs from expanding at an unrealistic growth rate when bNAbs are at relatively higher concentrations, we use

the Michaelis-Menten function $\frac{c_1 A}{c_2+A} ZI$ to depict the impact of bNAbs in triggering the proliferation of CTLs. This function has been widely used for this purpose in previous modeling studies [12, 50]. Here, c_1 and c_2 represent the maximum rate of CTL proliferation and their half-maximum saturation parameter, respectively. Finally, CTLs decay at a rate of d_6. All the parameters are positive constants, and we assume that $a + d_2 > b$, which is needed for the existence of the infected equilibrium.

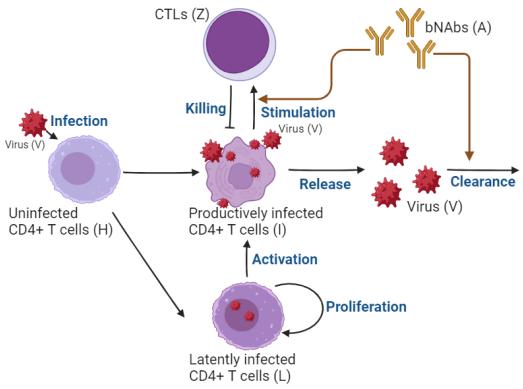

FIGURE 1. Schematic of the mathematical model of HIV dynamics with bNAbs and CTL immune response.

We will start with a simplified model by neglecting the term qAV in model (1), which represents the production of bNAbs stimulated by free virions. This omission is justified by the following considerations. First, according to the description in [5], the antibodies produced by the VIP experiment are very strong, making it reasonable to assume that bNAbs induced by VIP are much more potent than those induced by viruses. Second, neglecting the term qAV does not affect the main findings, as demonstrated by the numerical comparisons in Figs. 4 and 5. Lastly, including the virion stimulation of bNAbs complicates the mathematical analysis of the full model. Therefore, to simplify the mathematical analysis, we have omitted the term qAV in model (1). The simplified model is as follows:

$$\begin{cases} \dfrac{\mathrm{d}H(t)}{\mathrm{d}t} = \lambda - d_1 H - \beta(1-\varepsilon)HV, \\ \dfrac{\mathrm{d}L(t)}{\mathrm{d}t} = f(1-\varepsilon)\beta HV + bL - aL - d_2 L, \\ \dfrac{\mathrm{d}I(t)}{\mathrm{d}t} = (1-f)(1-\varepsilon)\beta HV + aL - d_3 I - pZI, \\ \dfrac{\mathrm{d}V(t)}{\mathrm{d}t} = Nd_3 I - d_4 V - mAV, \\ \dfrac{\mathrm{d}A(t)}{\mathrm{d}t} = r - d_5 A, \\ \dfrac{\mathrm{d}Z(t)}{\mathrm{d}t} = (c_0 + \dfrac{c_1 A}{c_2 + A})ZI - d_6 Z. \end{cases} \tag{2}$$

2.2. **Basic reproduction number and steady states.** The equilibrium of (2) satisfies

$$\begin{cases} \lambda - d_1 H - \beta(1-\varepsilon)HV = 0, \\ f(1-\varepsilon)\beta HV + bL - aL - d_2 L = 0, \\ (1-f)(1-\varepsilon)\beta HV + aL - d_3 I - pZI = 0, \\ Nd_3 I - d_4 V - mAV = 0, \\ r - d_5 A = 0, \\ (c_0 + \dfrac{c_1 A}{c_2 + A})ZI - d_6 Z = 0. \end{cases} \tag{3}$$

Obviously, there always exists an infection-free equilibrium $E_0 = (H_0, 0, 0, 0, A_0, 0) = (\frac{\lambda}{d_1}, 0, 0, 0, \frac{r}{d_5}, 0)$.

Using the next-generation method, the matrices for the new infection term $\mathbb{F}$ and the remaining transfer term $\mathbb{V}$ are given by:

$$\mathbb{F} = \begin{pmatrix} 0 & 0 & f(1-\varepsilon)\beta\frac{\lambda}{d_1} \\ 0 & 0 & (1-f)(1-\varepsilon)\beta\frac{\lambda}{d_1} \\ 0 & 0 & 0 \end{pmatrix}, \qquad \mathbb{V} = \begin{pmatrix} a+d_2-b & 0 & 0 \\ -a & d_3 & 0 \\ 0 & -Nd_3 & d_4 + m\frac{r}{d_5} \end{pmatrix}.$$

Thus, the basic reproduction number under treatment, $\mathcal{R}_0$, is computed to be:

$$\begin{aligned} \mathcal{R}_0 &= \rho(\mathbb{F}\cdot\mathbb{V}^{-1}) \\ &= \frac{\beta(1-\varepsilon)\lambda N d_5[a+(1-f)(d_2-b)]}{d_1(a+d_2-b)(d_4d_5+mr)}. \end{aligned} \tag{4}$$

When $\mathcal{R}_0 > 1$, in addition to the equilibrium E_0, system (2) has an infected equilibrium without CTL immune response $E_1 = (H_1, L_1, I_1, V_1, A_0, 0)$, where

$$\begin{aligned} H_1 &= \frac{\lambda}{d_1\mathcal{R}_0}, \\ L_1 &= \frac{\lambda f}{a+d_2-b}(1-\frac{1}{\mathcal{R}_0}), \\ I_1 &= \frac{d_1(d_4d_5+mr)}{d_3d_5N\beta(1-\varepsilon)}(\mathcal{R}_0-1), \\ V_1 &= \frac{d_1}{\beta(1-\varepsilon)}(\mathcal{R}_0-1). \end{aligned}$$

Define the CTL immune response reproduction number as

$$\mathcal{R}_c = \frac{\beta(1-\varepsilon)\lambda N d_5[a+(1-f)(d_2-b)][c_0c_2d_5+r(c_0+c_1)]}{(a+d_2-b)[d_1(d_4d_5+mr)(c_0c_2d_5+c_0r+c_1r)+\beta(1-\varepsilon)Nd_3d_5d_6(d_5c_2+r)]}.$$

If $\mathcal{R}_c > 1$, there exists an infected equilibrium with CTL immune response $E_2 = (H_2, L_2, I_2, V_2, A_0, Z_2)$, where

$$\begin{aligned} H_2 &= \frac{\lambda(d_4d_5+mr)[c_0c_2d_5+r(c_0+c_1)]}{d_1(d_4d_5+mr)[c_0c_2d_5+r(c_0+c_1)]+\beta(1-\varepsilon)Nd_3d_5d_6(d_5c_2+r)}, \\ L_2 &= \frac{1}{a+d_2-b}\cdot\frac{f\beta(1-\varepsilon)\lambda Nd_3d_5d_6(d_5c_2+r)}{d_1(d_4d_5+mr)[c_0c_2d_5+r(c_0+c_1)]+\beta(1-\varepsilon)Nd_3d_5d_6(d_5c_2+r)}, \\ I_2 &= \frac{d_6(r+c_2d_5)}{c_0c_2d_5+r(c_0+c_1)}, \end{aligned}$$

$$V_2 = \frac{Nd_3d_5d_6(c_2d_5 + r)}{(d_4d_5 + mr)[c_0c_2d_5 + r(c_0 + c_1)]},$$
$$Z_2 = \frac{d_3}{p}(\mathcal{R}_c - 1).$$

3. Stability analysis.

3.1. Local stability of E_0, E_1 and E_2.

To study the local stability of model (2) at $\tilde{E} = (\tilde{H}, \tilde{L}, \tilde{I}, \tilde{V}, \tilde{A}, \tilde{Z})$, where $\tilde{E}$ represents any of the equilibria E_0, E_1 and E_2, we linearize (2) and obtain the following Jacobian matrix

$$J(\tilde{E}) = \begin{pmatrix} -d_1 - \beta(1-\varepsilon)\tilde{V} & 0 & 0 & -\beta(1-\varepsilon)\tilde{H} & 0 & 0 \\ f(1-\varepsilon)\beta\tilde{V} & b-a-d_2 & 0 & f(1-\varepsilon)\beta\tilde{H} & 0 & 0 \\ (1-f)(1-\varepsilon)\beta\tilde{V} & a & -d_3 - p\tilde{Z} & (1-f)(1-\varepsilon)\beta\tilde{H} & 0 & -p\tilde{I} \\ 0 & 0 & Nd_3 & -d_4 - m\tilde{A} & -m\tilde{V} & 0 \\ 0 & 0 & 0 & 0 & -d_5 & 0 \\ 0 & 0 & c\tilde{Z} & 0 & \frac{c_1c_2}{(c_2+\tilde{A})^2}\tilde{Z}\tilde{I} & c\tilde{I} - d_6 \end{pmatrix}, \tag{5}$$

where

$$c = c_0 + \frac{c_1A_0}{c_2 + A_0}.$$

Theorem 3.1. *The infection-free equilibrium E_0 of the system is locally asymptotically stable when $\mathcal{R}_0 < 1$.*

Proof. Accroding to (5), the characteristic equation for E_0 can be written as

$$(\xi + d_5)(\xi + d_6)(\xi^3 + \alpha_1\xi^2 + \alpha_2\xi + \alpha_3) = 0 \tag{6}$$

in which

$$\alpha_1 = a + d_2 - b + d_3 + d_4 + mA_0,$$
$$\alpha_2 = d_3(a + d_2 - b) + (d_4 + mA_0)(a + d_2 - b + d_3) - Nd_3(1-f)\beta\frac{\lambda}{d_1},$$
$$\alpha_3 = (d_4 + mA_0)d_3(a + d_2 - b)(1 - \mathcal{R}_0).$$

Clearly, (6) has two negative eigenvalues $\xi_1 = -d_5$ and $\xi_2 = -d_6$. The remaining eigenvalues are determined by

$$\xi^3 + \alpha_1\xi^2 + \alpha_2\xi + \alpha_3 = 0.$$

Since $a + d_2 > b$ and $\mathcal{R}_0 < 1$, it is easy to verify that $\alpha_1 > 0,\ \alpha_3 > 0$ and

$$\begin{aligned} \alpha_1\alpha_2 - \alpha_3 &> (a + d_2 - b)((d_4 + mA_0)d_3 - Nd_3(1-f)\beta\frac{\lambda}{d_1}) \\ &\quad - (d_4 + mA_0)d_3(a + d_2 - b)(1 - \mathcal{R}_0) \\ &= af\beta\frac{\lambda}{d_1}Nd_3 \\ &> 0. \end{aligned}$$

Using the Routh-Hurwitz criterion, we conclude that all roots of (6) have negative real parts. Therefore, the infection-free equilibrium E_0 is locally asymptotically stable when $\mathcal{R}_0 < 1$. □

Similar to the proof of equilibrium E_0, by using the Routh-Hurwitz criterion, we have the following theorems on the local stability of the infected equilibrium without CTL immune response E_1 and the infected equilibrium with CTL immune response E_2. The proofs of theorems are based on algebraic calculations, which are given in "Appendices A and B".

Theorem 3.2. *If $\mathcal{R}_c < 1 < \mathcal{R}_0$, then the infected equilibrium without CTL immune response E_1 is locally asymptotically stable.*

Theorem 3.3. *If $\mathcal{R}_c > 1$, then the infected equilibrium with CTL immune response E_2 is locally asymptotically stable.*

3.2. **Global stability of E_0, E_1 and E_2.** In this section, we will examine the global stability of the equilibria of the model (2), which can be decoupled into

$$\begin{cases} \dfrac{\mathrm{d}H(t)}{\mathrm{d}t} = \lambda - d_1 H - \beta(1-\varepsilon)HV, \\ \dfrac{\mathrm{d}L(t)}{\mathrm{d}t} = f(1-\varepsilon)\beta HV + bL - aL - d_2 L, \\ \dfrac{\mathrm{d}I(t)}{\mathrm{d}t} = (1-f)(1-\varepsilon)\beta HV + aL - d_3 I - pZI, \\ \dfrac{\mathrm{d}V(t)}{\mathrm{d}t} = Nd_3 I - d_4 V - mAV, \\ \dfrac{\mathrm{d}Z(t)}{\mathrm{d}t} = (c_0 + \dfrac{c_1 A}{c_2 + A})ZI - d_6 Z, \end{cases} \tag{7}$$

and

$$\frac{\mathrm{d}A(t)}{\mathrm{d}t} = r - d_5 A. \tag{8}$$

It follows from (8) that

$$\lim_{t\to\infty} A(t) = \frac{r}{d_5} = A_0. \tag{9}$$

Substituting it into model (7) gives us the limiting system,

$$\begin{cases} \dfrac{\mathrm{d}H(t)}{\mathrm{d}t} = \lambda - d_1 H - \beta(1-\varepsilon)HV, \\ \dfrac{\mathrm{d}L(t)}{\mathrm{d}t} = f(1-\varepsilon)\beta HV + bL - aL - d_2 L, \\ \dfrac{\mathrm{d}I(t)}{\mathrm{d}t} = (1-f)(1-\varepsilon)\beta HV + aL - d_3 I - pZI, \\ \dfrac{\mathrm{d}V(t)}{\mathrm{d}t} = Nd_3 I - d_4 V - mA_0 V, \\ \dfrac{\mathrm{d}Z(t)}{\mathrm{d}t} = (c_0 + \dfrac{c_1 A_0}{c_2 + A_0})ZI - d_6 Z. \end{cases} \tag{10}$$

Theorem 3.4. *If $\mathcal{R}_0 < 1$, then the infected-free equilibrium E_0 is globally asymptotically stable.*

Proof. If $\mathcal{R}_0 < 1$, by Theorem 3.1, it follows that E_0 is locally asymptotically stable. Next, we only need to prove that E_0 is a global attractor of the system (2). Firstly, we prove that if $\mathcal{R}_0 < 1$, then the infected-free equilibrium $E_0^{\partial} = (\frac{\lambda}{d_1}, 0, 0, 0, 0)$

of the limiting system (10) is globally asymptotically stable. Define the following Lyapunov function

$$\begin{aligned}T_1(t) =&[af+(1-f)(a+d_2-b)](H-H_0-H_0\ln\frac{H}{H_0})+aL+(a+d_2-b)I\\&+\frac{[a+(1-f)(d_2-b)]\beta(1-\varepsilon)H_0}{d_4+mA_0}V+\frac{p(a+d_2-b)}{c}Z\end{aligned}$$

where $c=c_0+\frac{c_1A_0}{c_2+A_0}$. Then the time derivative of $T_1(t)$ along the solution of system (10) is

$$\begin{aligned}\frac{dT_1(t)}{dt} =&[af+(1-f)(a+d_2-b)](1-\frac{H_0}{H})[\lambda-d_1H-\beta(1-\varepsilon)HV]\\&+a[f(1-\varepsilon)\beta HV+bL-aL-d_2L]\\&+(a+d_2-b)[(1-f)(1-\varepsilon)\beta HV+aL-d_3I-pZI]\\&+\frac{[a+(1-f)(d_2-b)]\beta(1-\varepsilon)H_0}{d_4+mA_0}(Nd_3I-d_4V-mA_0V)\\&+\frac{p(a+d_2-b)}{c}(cZI-d_6Z)\\=&-[af+(1-f)(a+d_2-b)]\frac{d_1(H-H_0)^2}{H}+d_3(a+d_2-b)I(\mathcal{R}_0-1)\\&-\frac{p(a+d_2-b)d_6}{c}Z,\end{aligned}$$

where the equality $\lambda=d_1H_0$ has been used. Thus, $\frac{dT_1(t)}{dt}\le 0$ as $\mathcal{R}_0<1$. Further, if $\frac{dT_1(t)}{dt}=0$, we have $I=Z=0$ and $H=H_0$, which indicates $L=V=0$. Thus, the largest compact invariant set in $\{(H,L,I,V,Z):\frac{dT_1(t)}{dt}=0\}$ is the singleton set $\{E_0^\partial\}$. By LaSalle's Invariance Principle, we know that the infection-free equilibrium E_0^∂ of (10) is globally asymptotically stable when $\mathcal{R}_0<1$. Thus we get

$$\lim_{t\to\infty}H(t)=\frac{\lambda}{d_1},\qquad \lim_{t\to\infty}L(t)=\lim_{t\to\infty}I(t)=\lim_{t\to\infty}V(t)=\lim_{t\to\infty}Z(t)=0.$$

Since the system (10) is the limiting system of (2), from the Corollary 4.3 in [44], we further obtain that the infection-free equilibrium E_0 is the global attractor of the system (2). This completes the proof of the Theorem 3.4. □

Theorem 3.5. *If $\mathcal{R}_c<1<\mathcal{R}_0$, then the infected equilibrium without CTL immune response E_1 is globally asymptotically stable.*

Proof. Using similar arguments as those in the proof of Theorem 3.4, it suffices to show that the $E_1^\partial=(H_1,L_1,I_1,V_1,Z_1)$ of the limiting system (10) is globally asymptotically stable.

Define

$$\begin{aligned}T_2(t) =&[af+(1-f)(a+d_2-b)](H-H_1-H_1\ln\frac{H}{H_1})\\&+a(L-L_1-\ln\frac{L}{L_1})+(a+d_2-b)(I-I_1-I_1\ln\frac{I}{I_1})\\&+\frac{[af+(1-f)(a+d_2-b)]\beta(1-\varepsilon)H_1V_1}{Nd_3I_1}(V-V_1-\ln\frac{V}{V_1})\\&+\frac{p(a+d_2-b)}{c}Z.\end{aligned}$$

Calculating the time derivative of T_2 along the solutions of system (10) and using the steady state equalities $\lambda = d_1H_1+\beta(1-\varepsilon)H_1V_1$, $(a+d_2-b)L_1 = f(1-\varepsilon)\beta H_1V_1$, $d_3I_1 = (1-f)(1-\varepsilon)\beta H_1V_1 + aL_1$ and $Nd_3I_1 = d_4V_1 + mA_0V_1$, we can obtain

$$\begin{aligned}
\frac{dT_2}{dt} =&[af + (1-f)(a+d_2-b)]\\
&\times\left(\frac{-d_1(H-H_1)^2}{H} + (1-\varepsilon)\beta H_1V_1(1-\frac{H_1}{H}-\frac{HV}{H_1V_1}+\frac{V}{V_1})\right)\\
&+af(1-\varepsilon)\beta H_1V_1\left(\frac{HV}{H_1V_1}-\frac{L}{L_1}-\frac{HVL_1}{H_1V_1L}+1\right)\\
&+(a+d_2-b)\Bigg((1-f)(1-\varepsilon)\beta H_1V_1(\frac{HV}{H_1V_1}-\frac{I}{I_1}-\frac{HVI_1}{H_1V_1I}+1)\\
&+aL_1(\frac{L}{L_1}-\frac{I}{I_1}-\frac{LI_1}{L_1I}+1)+pI_1Z-PIZ\Bigg)\\
&+[af+(1-f)(a+d_2-b)]\beta(1-\varepsilon)H_1V_1(\frac{I}{I_1}-\frac{V}{V_1}-\frac{IV_1}{I_1V}+1)\\
&+\frac{p(a+d_2-b)}{c}(cZI-d_6Z)\\
=&-[af+(1-f)(a+d_2-b)]\frac{d_1(H-H_1)^2}{H}\\
&+[af+(1-f)(a+d_2-b)](1-\varepsilon)\beta H_1V_1(1-\frac{H_1}{H})\\
&+af(1-\varepsilon)\beta H_1V_1(-\frac{HVL_1}{H_1V_1L}+1)\\
&+(a+d_2-b)(1-f)(1-\varepsilon)\beta H_1V_1(-\frac{I}{I_1}-\frac{HVI_1}{H_1V_1I}+1)\\
&+(a+d_2-b)aL_1(-\frac{I}{I_1}-\frac{LI_1}{L_1I}+1)+(a+d_2-b)pI_1Z\\
&+[af+(1-f)(a+d_2-b)]\beta(1-\varepsilon)H_1V_1(\frac{I}{I_1}-\frac{IV_1}{I_1V}+1)\\
&-\frac{p(a+d_2-b)}{c}d_6Z\\
=&-[af+(1-f)(a+d_2-b)]\frac{d_1(H-H_1)^2}{H}\\
&+af(1-\varepsilon)\beta H_1V_1(4-\frac{H_1}{H}-\frac{HVL_1}{H_1V_1L}-\frac{IV_1}{I_1V}-\frac{LI_1}{L_1I})\\
&+(1-f)(1-\varepsilon)\beta H_1V_1(3-\frac{H_1}{H}-\frac{HVI_1}{H_1V_1I}-\frac{IV_1}{I_1V})\\
&+\frac{d_6(a+d_2-b)p}{c}(\mathcal{R}_c-1)Z.
\end{aligned}$$

When $\mathcal{R}_c < 1 < \mathcal{R}_0$, the inequality $\frac{dT_2(t)}{dt} \le 0$ holds and $\frac{dT_2(t)}{dt} = 0$ if and only if $H = H_1, L = L_1, I = I_1, V = V_1$ and $Z = 0$. Thus, the largest compact invariant set in $\{(H, L, I, V, Z) : \frac{dT_2(t)}{dt} = 0\}$ is the singleton set $\{E_1^\partial\}$. By LaSalle's Invariance Principle, we know that the infected equilibrium without equilibrium E_1^∂ of (10) is globally asymptotically stable when $\mathcal{R}_c < 1 < \mathcal{R}_0$, which completes the proof of the Theorem 3.5. □

Theorem 3.6. *If $\mathcal{R}_c > 1$, then the infected equilibrium with CTL immune response E_2 is globally asymptotically stable.*

Proof. Similarly to Theorems 3.4 and 3.5, we only need to show that the $E_2^\partial = (H_2, L_2, I_2, V_2, Z_2)$ of the limiting system (10) is globally asymptotically stable.

Let

$$\begin{aligned}
T_3(t) =&[af + (1-f)(a+d_2-b)](H - H_2 - H_2 \ln \frac{H}{H_2}) + a(L - L_2 - \ln \frac{L}{L_2}) \\
&+ (a + d_2 - b)(I - I_2 - I_2 \ln \frac{I}{I_2}) \\
&+ \frac{[af + (1-f)(a+d_2-b)]\beta(1-\varepsilon)H_2V_2}{Nd_3I_2}(V - V_2 - \ln \frac{V}{V_2}) \\
&+ \frac{p(a+d_2-b)}{c}(Z - Z_2 - Z_2 \ln \frac{Z}{Z_2}).
\end{aligned}$$

The time derivative of $T_3(t)$ along the solution of model (10) is given by

$$\begin{aligned}
\frac{dT_3(t)}{dt} =&[af + (1-f)(a+d_2-b)](1 - \frac{H_2}{H})(\lambda - d_1H - \beta(1-\varepsilon)HV) \\
&+ a(1 - \frac{L_2}{L})[f(1-\varepsilon)\beta HV + bL - aL - d_2L] \\
&+ (a + d_2 - b)(1 - \frac{I_2}{I})[(1-f)(1-\varepsilon)\beta HV + aL - d_3I - pZI] \\
&+ \frac{[af + (1-f)(a+d_2-b)]\beta(1-\varepsilon)H_2V_2}{Nd_3I_2}(1 - \frac{V_2}{V}) \\
&\times (Nd_3I - d_4V - mA_0V) + \frac{p(a+d_2-b)}{c}(1 - \frac{Z_2}{Z})(cIZ - d_6Z) \\
=& - [af + (1-f)(a+d_2-b)]\frac{d_1(H-H_2)^2}{H} \\
&+ [af + (1-f)(a+d_2-b)](1-\varepsilon)\beta H_2V_2 \\
&- [af + (1-f)(a+d_2-b)](1-\varepsilon)\beta H_2V_2\frac{H_2}{H} \\
&+ [af + (1-f)(a+d_2-b)](1-\varepsilon)\beta H_2V \\
&- af(1-\varepsilon)\beta\frac{HVL_2}{L} + af(1-\varepsilon)\beta H_2V_2 + af(1-\varepsilon)\beta\frac{H_2V_2L}{L_2} \\
&- (a + d_2 - b)d_3I - (a + d_2 - b)(1-f)(1-\varepsilon)\beta\frac{HVI_2}{I} \\
&- af(1-\varepsilon)\beta H_2V_2\frac{LI_2}{L_2I} + (a + d_2 - b)d_3I_2 \\
&+ [af + (1-f)(a+d_2-b)](1-\varepsilon)\beta H_2V_2\frac{I}{I_2} \\
&- [af + (1-f)(a+d_2-b)](1-\varepsilon)\beta H_2V \\
&- [af + (1-f)(a+d_2-b)](1-\varepsilon)\beta H_2V_2\frac{IV_2}{VI_2} \\
&+ [af + (1-f)(a+d_2-b)](1-\varepsilon)\beta H_2V_2 \\
&- p(a + d_2 - b)IZ_2 + p(a + d_2 - b)Z_2I_2 \\
=& - [af + (1-f)(a+d_2-b)]\frac{d_1(H-H_2)^2}{H}
\end{aligned}$$

$$+ af(1-\varepsilon)\beta H_2V_2(4-\frac{H_2}{H}-\frac{HVL_2}{H_2V_2L}-\frac{LI_2}{L_2I}-\frac{IV_2}{I_2V})$$
$$+ (a+d_2-b)(1-f)(1-\varepsilon)\beta H_2V_2(3-\frac{H_2}{H}-\frac{HVI_2}{H_2V_2I}-\frac{IV_2}{I_2V}),$$

where the equalities

$$\lambda = d_1H_2+\beta(1-\varepsilon)H_2V_2, \qquad Nd_3 = (d_4+mA_0)V_2,$$
$$d_3I_2+pI_2Z_2 = (1-f)(1-\varepsilon)\beta H_2V_2, \qquad (a+d_2-b)L_2 = f(1-\varepsilon)\beta H_2V_2$$

are used. Then the inequality $\frac{dT_3(t)}{dt} \leq 0$ holds and $\frac{dT_3(t)}{dt} = 0$ if and only if $H = H_2, L = L_2, I = I_2, V = V_2$ and $Z = Z_2$. Thus, the largest compact invariant set in $\{(H, L, I, V, Z) : \frac{dT_3(t)}{dt} = 0\}$ is the singleton set $\{E_2^\partial\}$. By LaSalle's Invariance Principle, we know that the infected equilibrium with CTL immune response E_2^∂ of (10) is globally asymptotically stable when $\mathcal{R}_c > 1$. This completes the proof of Theorem 3.6. □

4. Numerical simulations.

4.1. **Parameters.** To analyze the effect of bNAbs on viral dynamics, we fixed most of the parameter values of the model (2) based on experimental data and modeling literature [5,10,11,17,36,37,46,49]. For instance, the production rate of uninfected CD4+ T cells is $\lambda = 10^4\ ml^{-1}day^{-1}$ [36]. The death rates of target cells, latently and productively infected CD4+ T cells are 0.01 day^{-1}, 0.001 day^{-1}, and 1 day^{-1}, respectively [10,17]. Following Wang et al. [46], we fix the fraction of infection that leads to latency as $f = 0.001$. The viral infection rate of CD4+ T cells, denoted as β, is assumed to be $10^{-8} \sim 10^{-5}\ ml\ day^{-1}$ [11,37]. The clearance rate of productively infected cells by CTLs is $p = 0.05\ ml\ day^{-1}$ [49]. The production rate r of bNAbs by VIP is 100 $\mu g\ ml^{-1}day^{-1}$ based on experimental data [5]. The basal proliferation rate of CTLs is fixed at 0.01 day^{-1} [16]. The maximum proliferation rate of effector cells induced by bNAbs and their half-maximum saturation parameter are $c_1 = 0.01$ day^{-1} and $c_2 = 3\times10^{-5}\ ml^{-1}$ [12], respectively. The parameters in model (1) and their values are summarized in Table 1. We first perform simulations of the model (2) in the absence of drug and bNAb therapies and obtain the infected equilibrium with CTL immune response $(H, L, I, V, Z) = (9.58\times10^5, 415.7, 10, 8.7\times10^2, 820.8)$. These values are used as the initial states for simulating the model under drug therapy or bNAbs.

4.2. **Effects of drug and bNAb therapies.** In this subsection, we identify the influences of drug and bNAb therapies on the dynamics of model (2), respectively. Let $\beta = 8\times10^{-7}$ and take the other parameters from Table 1 with $\epsilon = 0.99$. It can be observed from Fig. 2(a) that the number of uninfected CD4+ T cells is high, indicating the effectiveness of all three treatments. Specifically, the number of uninfected CD4+ T cells is highest under combined drug and bNAb therapies, followed by drug therapy alone, with the lowest number observed under bNAb therapy alone. The opposite phenomenon can be observed in the dynamics of latently and productively infected CD4+ T cells (Figs. 2(b)(c)). It should be noted that to achieve a viral load below the detection limit at 3000 days, we assume a drug efficacy of 99%. However, if the drug efficacy decreases to 98%, the number of healthy cells treated with bNAb alone will exceed those treated with drug alone.

It can be seen from Fig. 2(d) that all three cases can rapidly reduce the virus. At day 3000, the viral loads for combination therapy, drug therapy, and bNAb

TABLE 1. Parameters and values used in model (1)

Parameter	Definition	Value and Unit	Sources
λ	Generation rate of uninfected CD4+ T cells	$10^4\ ml^{-1}day^{-1}$	[36]
d_1	Death rate of uninfected CD4+ T cells	$0.01\ day^{-1}$	[10, 17]
β	Infection rate of CD4+ T cells	$10^{-8} \sim 10^{-5}\ ml\ day^{-1}$	[11, 37]
f	Fraction of infection that leads to latency	0.001	[46]
b	Latent cell proliferation rate	$0.01\ day^{-1}$	[12]
a	Activation rate of latently infected cells	$0.01\ day^{-1}$	[11]
d_2	Death rate of latently infected cells	$0.001\ day^{-1}$	[10, 17]
d_3	Death rate of productively infected cells	$1\ day^{-1}$	[10, 17]
p	Clearance rate of productively infected cells by CTLs	$0.05\ ml\ day^{-1}$	[49]
N	Viral burst size	$2000\ virus\ cell^{-1}$	[11, 37]
d_4	Viral clearance rate	$23\ day^{-1}$	[17]
m	Neutralization rate of free viruses by bNAbs	$0.28\ day^{-1}$	[11]
r	Production rate of bNAbs by VIP	$100\ \mu g\ ml^{-1}day^{-1}$	[5]
q	Proliferation rate of bNAbs by viral stimulation	$0.001\ day^{-1}$	[18]
d_5	Death rate of bNAbs	$0.02\ day^{-1}$	[11]
c_0	Basal proliferation rate of CTLs	$0.01\ day^{-1}$	[16]
c_1	Max proliferation rate of CTLs induced by bNAbs	$0.01\ day^{-1}$	[12]
c_2	Half-maximum saturation parameter	$3 \times 10^{-5}\ ml^{-1}$	[12]
d_6	Death rate of CTLs	$1\ day^{-1}$	[12, 16]
ϵ	Overall drug efficacy of blocking virus infection	$[0, 1]$	See text

therapy are 0.3 RNA copies/ml, 63.35 RNA copies/ml, and 70.25 RNA copies/ml, respectively. Although Balazs et al. [5] found that VIP induces lifelong expression of bNAbs in humanized mice, it is more reasonable to assume that bNAbs may disappear over time. Therefore, in the simulation, we stop the bNAb therapy at day 3000 to model the disappearance of bNAbs within the host and simultaneously discontinue the drug therapy. Unfortunately, the viral load rebounds to levels above the detection limit after bNAb or drug therapy is terminated. Following [12], we set the detection limit of viral load as 100 RNA copies/ml. To further understand the viral rebound, we consider the 5 days before the end of treatment to 35 days after treatment, i.e., days $2995 - 3035$, shown in Fig. 2(f). For drug therapy alone, the rebound time is less than one day. When only bNAb therapy is administered, the rebound time is 4 days. This indicates that bNAb therapy delays the viral rebound time. The rebound time extends to 35 days when the joint therapy of both bNAb and drug is adopted. This result is inevitable because combination therapy drives the viral load to a lower level. This finding confirms the potential role of bNAbs in controlling virus production.

We observe in Fig. 2(c) that the productively infected CD4+ T cells ultimately decrease to zero under combination therapy and drug therapy alone. This indicates that the CTL immune response cannot be effectively activated in these two scenarios, as depicted in Fig. 2(e). However, bNAb therapy alone can successfully trigger the CTL immune response, aligning with findings in [13, 32, 33, 38]. In summary, bNAb therapy can increase the population of uninfected CD4+ T cells, decrease the number of infected cells, activate the CTL immune response, and delay the viral rebound time, thus emerging as a promising treatment option.

4.3. **The influence on viral reduction.** In addition to drug treatment, bNAbs and the CTL immune response can also contribute to reducing the viral load. From Fig. 2(d), we observe that the viral load is suppressed below the detection limit

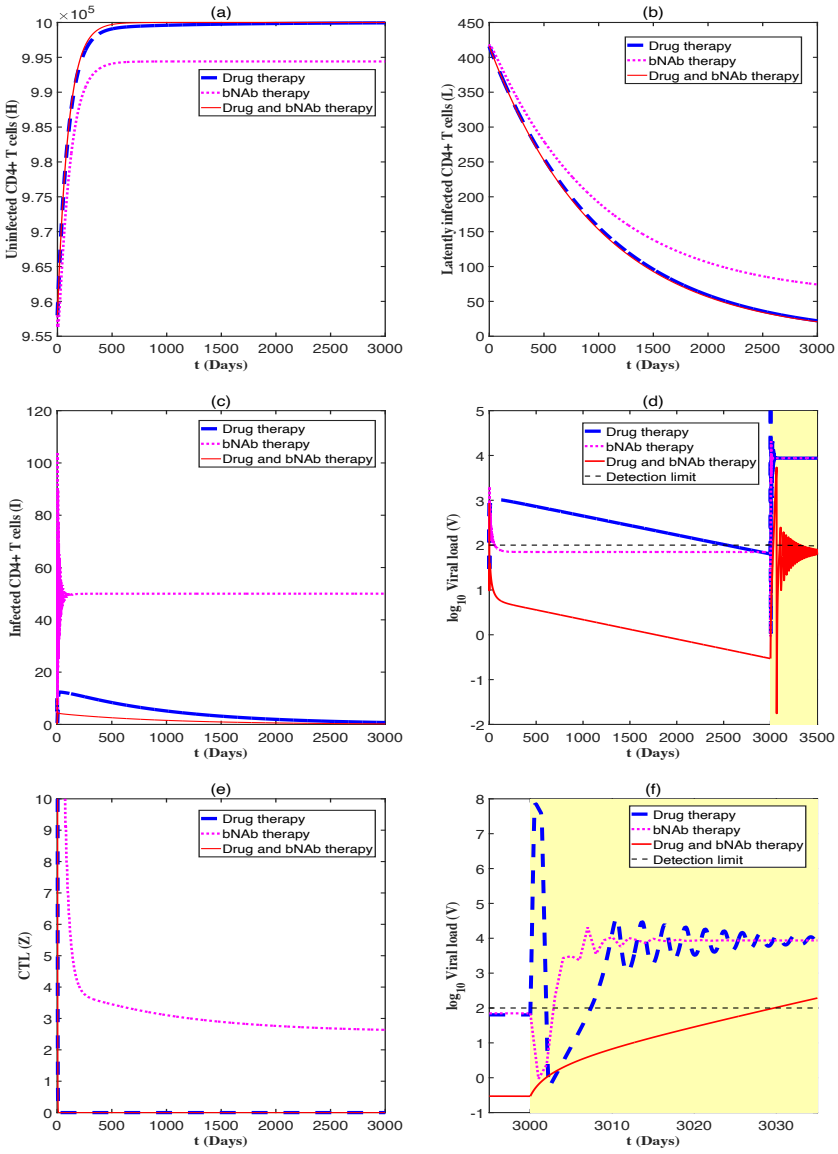

FIGURE 2. The dynamics of uninfected cells (a), infected cells (b,c), viral load (d,f), and CTLs (e) under different treatment measures. Black dashed lines in (d) and (f) indicate the viral load detection limit (100 RNA copies/mL). In (d) and (f), the shaded yellow box shows the time periods of stopping drug and bNAb therapies. Parameter values used are in Table 1 with $\beta = 8 \times 10^{-7}$ and $\epsilon = 0.99$. Under combined drug and bNAb therapies, the basic reproduction number is $\mathcal{R}_0 = 0.01$, and the CTL immune response reproduction number is $\mathcal{R}_c = 0.01$. For bNAb therapy alone, $\mathcal{R}_0$ and $\mathcal{R}_c$ are 1.135 and 1.128, respectively.

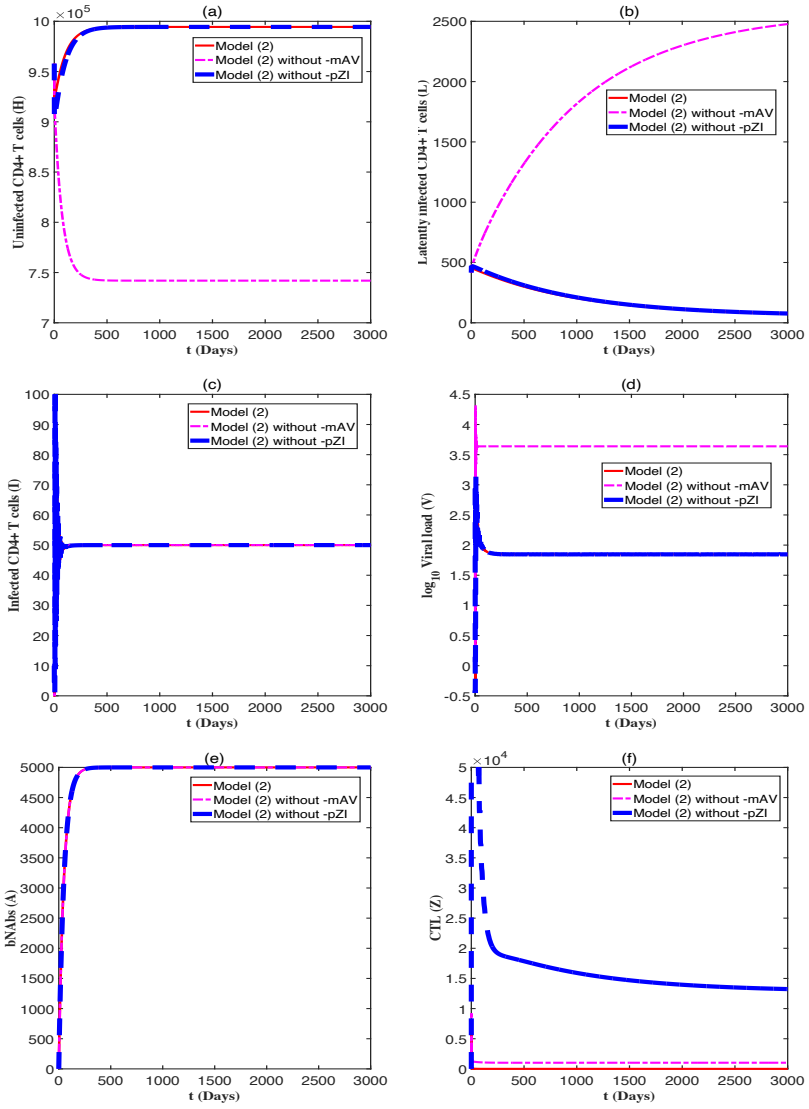

FIGURE 3. Comparison of the dynamics predicted by model (2), model (2) without $-pZI$, and model (2) without $-mAV$. (a)-(e) The inclusion of the clearance of productively infected cells by CTLs ($-pZI$) does not alter the dynamics of uninfected cells, infected cells, viral load, and bNAbs. However, neglecting the neutralization of free viruses ($-mAV$) results in fewer uninfected cells, higher levels of latently infected cells, and virus. This indicates that bNAb therapy has a greater impact on viral control than the CTL immune response. (f) The dynamics of CTLs under different scenarios. For model (2), model (2) without the term $-pZI$, and model (2) without the term $-mAV$, the basic reproduction numbers are 1.135, 1.135, and 70.2, respectively. The corresponding CTL immune response reproduction numbers are 1.128, 1.128, and 52.08, respectively.

and persists at a low level for an extended period through bNAb therapy alone, obviating the need for lifelong drug therapy. This outcome aligns well with in vivo experimental results [6,14,15,34]. Thus, to isolate the effects of bNAbs and the CTL immune response on HIV infection and eliminate the influence of drug therapy, we set the overall drug efficacy in inhibiting virus infection, ϵ, to 0. In our model, free viruses are neutralized by bNAbs, and productively infected cells are cleared by the CTL immune response, represented as $-mAV$ and $-pZI$, respectively. We now investigate how these factors affect the dynamics of the virus and cells.

Figure 3 shows the changes in uninfected cells, latent reservoir, productively infected cells, viral load, bNAbs, and CTLs. In Fig. 3(a)-(e), the curves of model (2) with and without $-pZI$ overlap. This indicates that removing the clearance term of CTLs on productively infected cells does not visibly affect the dynamics of uninfected cells, infected cells, viral load, and bNAbs. Compared to model (2), the model without $-mAV$ exhibits fewer uninfected cells, higher levels of latently infected cells, and virus. These results suggest that bNAbs have a more significant impact on viral control than the CTL immune response.

From Fig. 3(f), we observe that model (2) without $-pZI$ exhibits the highest abundance of CTLs, followed by the model (2) without $-mAV$, and finally, the model (2). This is reasonable because, according to model (2), the loss of CTLs occurs through two pathways: one is basal death d_6Z, and the other is killing infected cells $-pZI$. Excluding the clearance of productively infected cells by CTLs can result in a reduction in CTL losses, leading to maximum CTL levels. However, when both $-pZI$ and $-mAV$ are included, the neutralization of free viruses consumes bNAbs, decreasing the production of the CTL immune response. This, coupled with the loss of CTLs by killing infected cells, results in lower CTL levels compared to model (2) without $-mAV$. Based on these findings, we speculate that the enhanced antigenicity by bNAbs could be a significant source of CTLs. This will be validated in the following section.

4.4. **The generation of CTL immune response.** There are two pathways contributing to the CTL immune response: one is through the activation of other antigens, and the other is through bNAbs. For comparison, we plot model (2) without CTL immune response in Fig. 4. We find that model (2) without CTLs has the lowest steady-state uninfected CD4+ T cells compared to model (2) with CTLs, i.e., model (2) and model (2) without bNAb activation (see Fig. 4(a)). In Figs. 4(b)-(d), when considering bNAb activation in the CTL immune response (i.e., model (2)), the levels of infected cells (latently and productively infected cells) and viruses are the lowest. If model (2) does not include bNAb activation or CTLs, the levels of infected cells and viruses increase. Moreover, model (2) without CTL immune response has a higher viral load and infected cells compared to model (2) with CTL immune response. These results demonstrate that the inclusion of CTL immune response can generate a higher level of uninfected CD4+ T cells and significantly reduce infected cells and viral load.

From Fig. 4(e), it can be observed that the CTL immune response initially decreases and then stabilizes in both cases to lyse infected cells. If there is enhanced antigenicity by bNAbs in the model, the level of CTLs is higher, indicating that bNAbs can increase the CTL immune response, consistent with the results in Fig. 3(f). To provide further information on the CTL immune response, we evaluate the relative contributions from other antigens and bNAbs, which are given by the

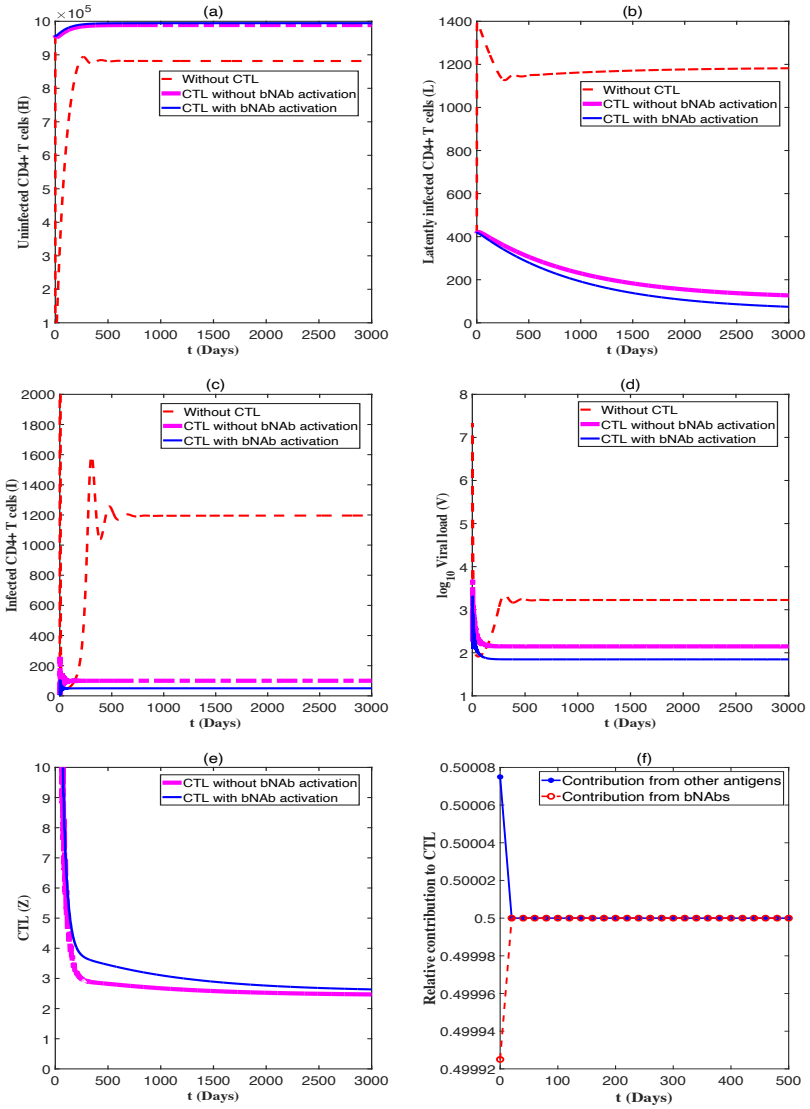

FIGURE 4. The effects of CTL immune response and bNAb activation, i.e., $\frac{c_1 A}{c_2+A} ZI$, on the dynamics of model (2). (a)-(d) CTL immune response increases the level of uninfected CD4+ T cells and significantly reduces infected cells (both latently and productively infected) and viral load. (e) The effect of enhanced antigenicity by bNAbs on the CTL immune response. In this case, the CTL immune response is enhanced due to bNAbs. (f) The relative contributions to the CTL immune response from other antigens and bNAbs. Under CTL without bNAb activation, the basic reproduction number is $\mathcal{R}_0 = 1.135$ and the CTL immune response reproduction number is $\mathcal{R}_c = 1.122$. In the case of CTL with bNAb activation, the reproduction numbers are the same as those in model (2).

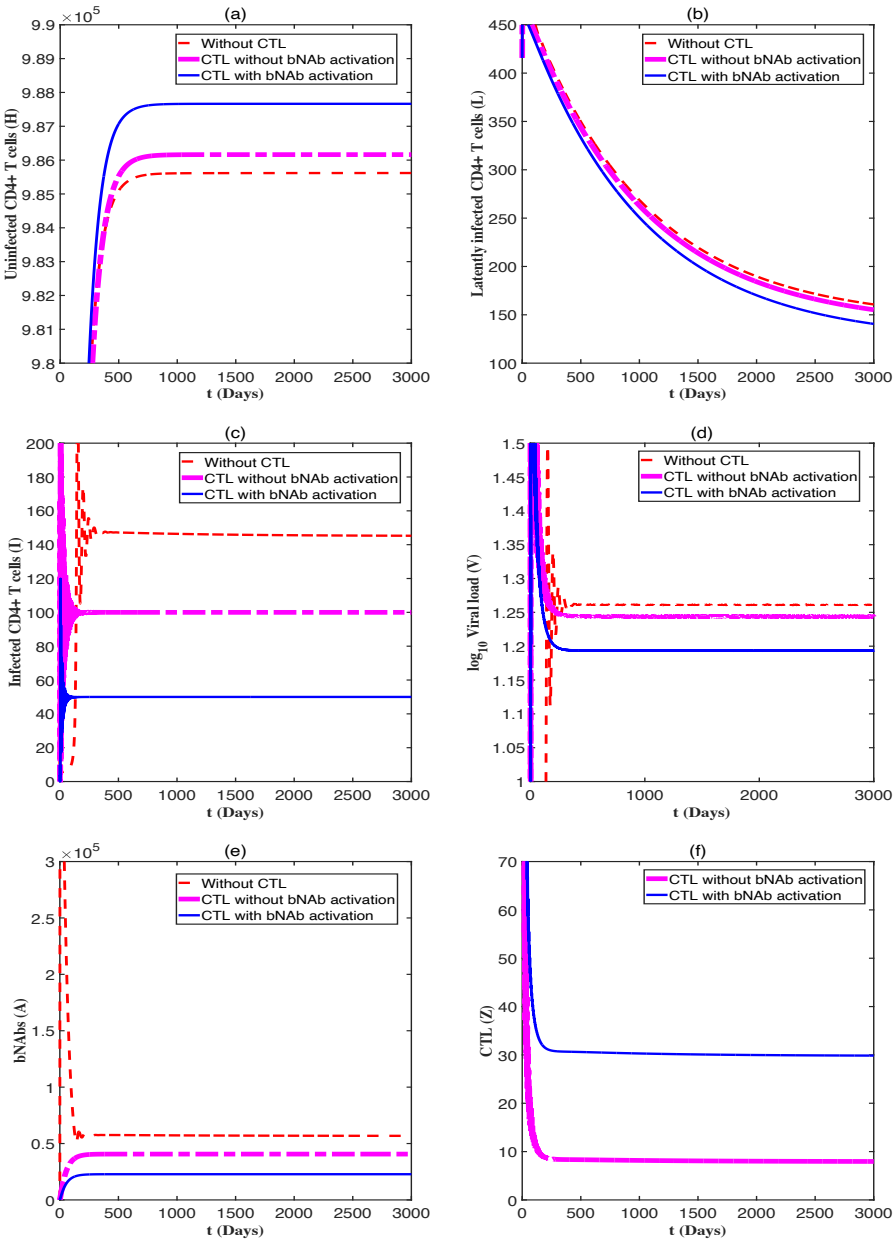

FIGURE 5. Effect of including the proliferation of bNAbs by viral stimulation on dynamics. We choose $\beta = 8 \times 10^{-6}$ and the other parameters are the same as those in Fig. 4.

following two ratios:

$$\frac{c_0}{c_0 + \frac{c_1 A}{c_2 + A}} \quad \text{and} \quad \frac{\frac{c_1 A}{c_2 + A}}{c_0 + \frac{c_1 A}{c_2 + A}}.$$

As described in Fig. 4(f), during the first 20 days of infection, the relative contribution from other antigens decreases, whereas the contribution from bNAbs increases. As the infection progresses, model (2) eventually converges to the infected equilibrium with CTL immune response. Thus, two curves representing the relative contributions to CTL immune response also converge to constant values. Interestingly, the relative contributions of the two sources for CTLs are the same. This result suggests that the activation of bNAb plays a critical role in the establishment of CTL immune response.

In the previous sections, we numerically studied the dynamics of model (2), which omitted the term qAV from model (1), i.e., the proliferation of bNAbs by viral stimulation. In the following, we incorporate qAV into model (2). It's worth noting that the inclusion of the term qAV increases the bNAbs, resulting in a reduction of viral load, which consequently decreases infected CD4+ T cells. This, coupled with the observations in Fig. 4(e), suggests that the CTL immune response may not be successfully activated. To address this, we increase the infection rate of the virus from 8×10^{-7} to 8×10^{-6} to elevate the viral load. The other parameters remain unchanged as in Fig. 4. From Fig. 5, we observe that although the quantities of cells and viruses differ from those in Fig. 4, the conclusion remains consistent, indicating that the proliferation of bNAbs by viral stimulation, qAV, does not alter our findings.

5. **Discussion.** In the early 1990s, first-generation bNAbs were isolated, including 2F5, 2G12, Z13, and 4E10. They are deemed safe and have demonstrated the ability to reduce viral load in HIV-infected individuals [2, 43]. The development of single-cell antibody cloning techniques [45] and viral neutralization assays [31] led to the isolation of second-generation bNAbs with improved potency and neutralization breadth [23]. However, rapid viral resistance and escape are often observed in bNAb monotherapy [3]. Similar to the development of antiretroviral medications, a combination of multiple bNAbs significantly reduces the likelihood of HIV escape and resistance [14, 23], thereby minimizing the risk of immunotherapeutic failure. Recently, bNAbs have been shown to provide high protection against HIV/SHIV infection by inducing persistent immunity in the host [32–34]. cART has been widely used in the treatment and prevention of HIV-infected patients. To date, treatment with bNAbs has not been directly compared to cART to assess their relative efficacy, nor have investigations been conducted into the potential efficacy of combined bNAbs and cART.

In this study, we employ mathematical modeling to examine the effects of bNAb therapy and cART on viral dynamics. In the model, bNAbs are assumed to control HIV infection by neutralizing viruses and activating CTL immune responses through enhanced antigen presentation. Therefore, we also explore the mechanisms underlying viral control by bNAbs as well as the CTL immune response. The dynamics of the model have been thoroughly analyzed by demonstrating the global stability of all possible equilibria. Our numerical analyses suggest that treatment with bNAbs alone or in combination with antiretroviral drugs can significantly reduce viral load and delay viral rebound when treatment is discontinued (see Figs. 2(d)(f)). In Fig. 3, we compare the dynamics predicted by model (2), model (2) without $-mAV$ (i.e., the neutralization of viruses by bNAbs), and model (2) without $-pZI$ (i.e., the clearance of productively infected cells by CTLs). We find that bNAbs have a larger impact on viral control than the CTL immune response. When

CTL immune responses are taken into consideration, the population of uninfected cells increases, accompanied by a decline in the levels of infected cells and viruses (Figs. 3(a-d)). This result underscores the importance of the CTL immune response, which should not be overlooked in studying HIV infection dynamics. When bNAb activation (i.e., $\frac{c_1 A}{c_2+A} ZI$) exists, the level of CTLs is high (see Figs. 2(e), 3(f), and 4(e)). Further analysis of the relative contributions to the CTL immune response shows that activation of bNAbs accounts for half of the CTLs (Fig. 4(f)).

For the case of $q \neq 0$ (i.e., model (1)), a rigorous theoretical analysis is challenging, including deriving explicit expressions for all equilibria and their stability. We speculate that the existence of equilibria depends on conditions beyond the reproduction numbers. The influence of the neglected term qAV in the simplified model has been evaluated using numerical simulations (Fig. 5). From Fig. 5, it can be seen that under the current parameters, the solutions of the full model (1) (i.e., CTL with bNAb activation) converge to the infected equilibrium with CTL immune response. For the cases where $-pZI$ and $-mAV$ are removed, these are equivalent to the cases of $p = 0$ and $m = 0$ in model (2), respectively. Thus, the theoretical analysis presented in this article is fully applicable to these two special cases.

It is worth mentioning that when bNAb therapy is administered, viral load becomes undetectable, but viremia will resurge if bNAbs are absent (Fig. 2(d)). In other words, viremia would rebound when the level of administered bNAbs in circulation diminishes. Thus, the half-life of an antibody is crucial for determining the therapeutic outcome and efficacy of bNAbs. Increasing antibody half-life may enhance the killing of latently infected cells and prolong effective viral suppression. Several strategies have been adopted to further extend the antibody's half-life without impairing its functionality in vivo. One feasible method is to modify the Fc domain to have a higher affinity for the neonatal Fc receptor [27, 39]. For nanobodies and scFvs that do not have an Fc domain, the addition of polyethylene glycol or albumin has been explored to extend the expression of bNAbs for a longer period [22,30]. Other half-life extension methods, such as recombinant adeno-associated virus vectors and gene transfer technologies, have significantly extended the lifetime of bNAbs [4, 5].

In addition to cell-free infection, direct cell-to-cell transmission is another mechanism by which HIV infects target cells. Cell-to-cell transmission is primarily mediated through virological synapses, which allow multiple infections of target cells without exposure to an external environment [17]. This leads to rapid and efficient virus spread [9,17]. The efficacy of bNAbs in inhibiting cell-to-cell transmission has been assessed, but the conclusions vary and can even be conflicting, depending on virus strains, assay systems, and the mode of action [28, 29, 35]. Thus, it would be of great interest to study the capacities of bNAbs against cell-free virus infection and cell-to-cell transmission through mathematical modeling in future studies.

Acknowledgments. T. Guo is supported by the Changzhou Scientific and Technological Program grant (CJ20220134), the fourth series of leading projects to introduce and cultivate innovative talents in Changzhou (CQ20230111), the Natural Science Foundation of Jiangsu Higher Education (22KJB110007), and the National Natural Science Foundation of China (12201077). S. Gao is supported by the National Natural Science Foundation of China (12301629), and the overseas talents urgently needed in Jiangxi Province (20232BCJ25045). Z. Qiu is supported by the

National Natural Science Foundation of China (12071217). L. Rong is supported by the NSF grants DMS-1950254 and DMS-2324692.

Appendix A - Proof of Theorem 3.2. From (5), the Jacobian matrix of model (2) at E_1 is

$$J(E_1) = \begin{pmatrix} J_{11} & J_{12} \\ 0 & J_{22} \end{pmatrix}, \tag{11}$$

where

$$J_{11} = \begin{pmatrix} -d_1 - \beta(1-\varepsilon)V_1 & 0 & 0 & -\beta(1-\varepsilon)H_1 \\ f(1-\varepsilon)\beta V_1 & b-a-d_2 & 0 & f(1-\varepsilon)\beta H_1 \\ (1-f)(1-\varepsilon)\beta V_1 & a & -d_3 & (1-f)(1-\varepsilon)\beta H_1 \\ 0 & 0 & Nd_3 & -d_4 - mA_0 \end{pmatrix},$$

and

$$J_{12} = \begin{pmatrix} 0 & 0 \\ 0 & 0 \\ 0 & -pI_1 \\ -mV_1 & 0 \end{pmatrix}, \qquad J_{22} = \begin{pmatrix} -d_5 & 0 \\ 0 & cI_1 - d_6 \end{pmatrix}.$$

Define $\Upsilon(J)$ as the set of eigenvalues generated by matrix J. We have $\Upsilon(J) = \Upsilon(J_{11}) \cup \Upsilon(J_{22})$.

The characteristic equation associated with J_{22} at E_1 is given by

$$(\xi + d_5)(\xi - cI_1 + d_6) = 0, \tag{12}$$

where ξ is the eigenvalue. It is easy to see that (12) has a negative eigenvalue $\xi_1 = -d_5$. Substituting the equalities $c = c_0 + \frac{c_1 A_0}{c_2 + A_0}$, $I_1 = \frac{d_1(d_4 d_5 + mr)}{d_3 d_5 N\beta(1-\varepsilon)}(\mathcal{R}_0 - 1)$ and $\mathcal{R}_0 = \frac{\beta(1-\varepsilon)\lambda N d_5[a+(1-f)(d_2-b)]}{d_1(a+d_2-b)(d_4 d_5 + mr)}$ into (12), we have

$$\xi_2 = \frac{d_1(d_4 d_5 + mr)(c_0 c_2 d_5 + c_0 r + c_1 r) + \beta(1-\varepsilon)N d_3 d_5 d_6(d_5 c_2 + r)}{d_3 d_5 N\beta(1-\varepsilon)(c_2 d_5 + r)}(\mathcal{R}_c - 1).$$

Because $R_c < 1$, the inequality $\xi_2 < 0$ holds. Thus, the roots of (12) are all negative. The local stability of the equilibrium E_1 is determined by the eigenvalues of the matrix J_{11}. The characteristic equation of J_{11} is

$$\begin{aligned} &(\xi - b + a + d_2)(\xi + d_3)(\xi + d_4 + mA_0)[\xi + d_1 + \beta(1-\varepsilon)V_1] \\ &-(\xi + d_1)(\xi - b + a + d_2)(1-f)(1-\varepsilon)N d_3 \beta H_1 \\ &+[\xi + d_1 + \beta(1-\varepsilon)V_1] f(1-\varepsilon) a N d_3 \beta H_1 + a N d_3 f \beta^2 (1-\varepsilon)^2 H_1 V_1 \\ &=0. \end{aligned} \tag{13}$$

Using the equalities $(1-f)(1-\varepsilon)\beta H_1 V_1 + aL_1 = d_3 I_1$ and $Nd_3 I_1 = d_4 V_1 + mA_0 V_1$, Eq. (13) can be written as

$$\xi^4 + a_1\xi^3 + a_2\xi^2 + a_3\xi + a_4 = 0,$$

where

$$\begin{aligned} a_1 &= d_1 + \beta(1-\varepsilon)V_1 + a + d_2 - b + d_3 + d_4 + mA_0, \\ a_2 &= (a + d_2 - b)(d_4 + mA_0) + d_3(a + d_2 - b) + (d_4 + mA_0)[d_1 + \beta(1-\varepsilon)V_1] \\ &\quad + d_3[d_1 + \beta(1-\varepsilon)V_1] + (a + d_2 - b)[d_1 + \beta(1-\varepsilon)V_1] + \frac{a(d_4 + mA_0)L_1}{I_1}, \\ a_3 &= d_3(d_4 + mA_0)\beta(1-\varepsilon)V_1 + (a + d_2 - b)(d_4 + mA_0)[d_1 + \beta(1-\varepsilon)V_1] \end{aligned}$$

$$
\begin{aligned}
&+ d_3(a+d_2-b)[d_1+\beta(1-\varepsilon)V_1] + aNd_3f(1-\varepsilon)\beta H_1\\
&+ \frac{a(a+d_2-b)(d_4+mA_0)L_1}{I_1} + \frac{ad_1(d_4+mA_0)L_1}{I_1},\\
a_4 &= d_3(d_4+mA_0)(a+d_2-b)\beta(1-\varepsilon)V_1 + aNd_3f(1-\varepsilon)\beta H_1[d_1+\beta(1-\varepsilon)V_1]\\
&+ aNd_3f(1-\varepsilon)^2\beta^2H_1V_1 + \frac{ad_1(a+d_2-b)(d_4+mA_0)L_1}{I_1}.
\end{aligned}
$$

Since $\mathcal{R}_0 > 1$, we obtain that $L_1, I_1, V_1 > 0$. Thus, $a_1, a_2, a_3, a_4 > 0$. Moreover, we have

$$
\begin{aligned}
\triangle_2 &= a_1a_2 - a_3\\
&= d_1\Bigg((a+d_2-b)(d_4+mA_0) + (d_4+mA_0)[d_1+\beta(1-\varepsilon)V_1]\\
&\quad + d_3[d_1+\beta(1-\varepsilon)V_1] + (a+d_2-b)[d_1+\beta(1-\varepsilon)V_1]\Bigg)\\
&\quad + \beta(1-\varepsilon)V_1\Bigg((a+d_2-b)(d_4+mA_0) + (d_4+mA_0)[d_1+\beta(1-\varepsilon)V_1]\\
&\quad + d_3[d_1+\beta(1-\varepsilon)V_1] + (a+d_2-b)[d_1+\beta(1-\varepsilon)V_1] + \frac{a(d_4+mA_0)L_1}{I_1}\Bigg)\\
&\quad + (a+d_2-b)\Bigg((a+d_2-b)(d_4+mA_0) + d_3(a+d_2-b)\\
&\quad + (d_4+mA_0)[d_1+\beta(1-\varepsilon)V_1] + d_3[d_1+\beta(1-\varepsilon)V_1]\\
&\quad + (a+d_2-b)[d_1+\beta(1-\varepsilon)V_1]\Bigg)\\
&\quad + d_3\Bigg((a+d_2-b)(d_4+mA_0) + d_3(a+d_2-b)\\
&\quad + (d_4+mA_0)[d_1+\beta(1-\varepsilon)V_1] + d_3[d_1+\beta(1-\varepsilon)V_1] + (a+d_2-b)\\
&\quad \times [d_1+\beta(1-\varepsilon)V_1] + \frac{a(d_4+mA_0)L_1}{I_1}\Bigg)\\
&\quad + (d_4+mA_0)\Bigg((a+d_2-b)(d_4+mA_0) + d_3(a+d_2-b)\\
&\quad + (d_4+mA_0)[d_1+\beta(1-\varepsilon)V_1] + d_1d_3 + \frac{a(d_4+mA_0)L_1}{I_1}\Bigg)\\
&\quad - aNd_3f(1-\varepsilon)\beta H_1.
\end{aligned}
$$

Using the equalities $f(1-\varepsilon)\beta H_1V_1 + bL_1 = aL_1 + d_2L_1$, $Nd_3I_1 = d_4V_1 + mA_0V_1$, $L_1 = \frac{\lambda f}{a+d_2-b}(1-\frac{1}{\mathcal{R}_0})$, $I_1 = \frac{d_1(d_4d_5+mr)}{d_3d_5N\beta(1-\varepsilon)}(\mathcal{R}_0-1)$ and $\mathcal{R}_0 = \frac{\beta(1-\varepsilon)\lambda Nd_5[a+(1-f)(d_2-b)]}{d_1(a+d_2-b)(d_4d_5+mr)}$, we derive

$$
-aNd_3f(1-\varepsilon)\beta H_1 = -\frac{af}{a+(1-f)(d_2-b)}d_3(a+d_2-b)(d_4+mA_0).
$$

Since $(1-f)(a+d_2-b) > 0$, we have $\frac{af}{a+(1-f)(d_2-b)} < 1$, which implies that $d_3(a+d_2-b)(d_4+mA_0) - \frac{af}{a+(1-f)(d_2-b)} d_3(a+d_2-b)(d_4+mA_0) > 0$. Thus, $\triangle_2 > 0$.

From this, we get

$$
\begin{aligned}
\triangle_3 =& a_3\triangle_2 - a_1^2 a_4 \\
=& \Bigg\{ d_3(d_4+mA_0)\beta(1-\varepsilon)V_1 + (a+d_2-b)(d_4+mA_0)[d_1+\beta(1-\varepsilon)V_1] \\
& + d_3(a+d_2-b)[d_1+\beta(1-\varepsilon)V_1] + aNd_3f(1-\varepsilon)\beta H_1 \\
& + \frac{a(a+d_2-b)(d_4+mA_0)L_1}{I_1} + \frac{ad_1(d_4+mA_0)L_1}{I_1} \Bigg\} \\
& \times \Bigg\{ d_1 \Bigg((a+d_2-b)(d_4+mA_0) + (d_4+mA_0)[d_1+\beta(1-\varepsilon)V_1] \\
& + d_3[d_1+\beta(1-\varepsilon)V_1] + (a+d_2-b)[d_1+\beta(1-\varepsilon)V_1] \Bigg) \\
& + \beta(1-\varepsilon)V_1 \Bigg((a+d_2-b)(d_4+mA_0) + (d_4+mA_0) \\
& \times [d_1+\beta(1-\varepsilon)V_1] + d_3[d_1+\beta(1-\varepsilon)V_1] \\
& + (a+d_2-b)[d_1+\beta(1-\varepsilon)V_1] + \frac{a(d_4+mA_0)L_1}{I_1} \Bigg) \\
& + (a+d_2-b) \Bigg((a+d_2-b)(d_4+mA_0) + d_3(a+d_2-b) \\
& + (d_4+mA_0)[d_1+\beta(1-\varepsilon)V_1] \\
& + d_3[d_1+\beta(1-\varepsilon)V_1] + (a+d_2-b)[d_1+\beta(1-\varepsilon)V_1] \Bigg) \\
& + d_3 \Bigg((a+d_2-b)(d_4+mA_0) + d_3(a+d_2-b) \\
& + (d_4+mA_0)[d_1+\beta(1-\varepsilon)V_1] + d_3[d_1+\beta(1-\varepsilon)V_1] + (a+d_2-b) \\
& \times [d_1+\beta(1-\varepsilon)V_1] + \frac{a(d_4+mA_0)L_1}{I_1} \Bigg) \\
& + (d_4+mA_0) \Bigg((a+d_2-b)(d_4+mA_0) + d_3(a+d_2-b) \\
& + (d_4+mA_0)[d_1+\beta(1-\varepsilon)V_1] + d_1d_3 + \frac{a(d_4+mA_0)L_1}{I_1} \Bigg) \\
& - aNd_3f(1-\varepsilon)\beta H_1 \Bigg\} - \Big(d_1+\beta(1-\varepsilon)V_1 + a + d_2 - b + d_3 + d_4 + mA_0 \Big) \\
& \times \Big(d_1+\beta(1-\varepsilon)V_1 + a + d_2 - b + d_3 + d_4 + mA_0 \Big) \Big\{ d_3(d_4+mA_0)
\end{aligned}
$$

$$\times (a+d_2-b)\beta(1-\varepsilon)V_1 + aNd_3f(1-\varepsilon)\beta H_1[d_1+\beta(1-\varepsilon)V_1]$$
$$+ aNd_3f(1-\varepsilon)^2\beta^2H_1V_1 + \frac{ad_1(a+d_2-b)(d_4+mA_0)L_1}{I_1}\Bigg\}.$$

Through lengthy algebraic calculations, all the negative terms on the right-hand side of the above equation can be eliminated, thus the inequality $\triangle_3 > 0$ holds. This, together with the inequality $a_4 > 0$, implies that $\triangle_4 = a_4\triangle_3 > 0$. Therefore, it follows from the Routh-Hurwitz criterion that all roots of (13) have negative real parts. Thus, the equilibrium E_1 is locally asymptotically stable when $\mathcal{R}_c < 1 < \mathcal{R}_0$.

Appendix B - Proof of Theorem 3.3. Calculating the Jacobian matrix of (2) at E_2, we have

$$J(E_2) = \begin{pmatrix} -d_1-\beta(1-\varepsilon)V_2 & 0 & 0 & -\beta(1-\varepsilon)H_2 & 0 & 0 \\ f(1-\varepsilon)\beta V_2 & b-a-d_2 & 0 & f(1-\varepsilon)\beta H_2 & 0 & 0 \\ (1-f)(1-\varepsilon)\beta V_2 & a & -d_3-pZ_2 & (1-f)(1-\varepsilon)\beta H_2 & 0 & -pI_2 \\ 0 & 0 & Nd_3 & -d_4-mA_0 & -mV_2 & 0 \\ 0 & 0 & 0 & 0 & -d_5 & 0 \\ 0 & 0 & cZ_2 & 0 & \frac{c_1c_2}{(c_2+A_0)^2}Z_2I_2 & 0 \end{pmatrix}. \tag{14}$$

From this, the characteristic equation is given by

$$\begin{aligned}&(\xi+d_5)\Big\{\xi(\xi+d_4+mA_0)[\xi+d_1+\beta(1-\varepsilon)V_2](\xi-b+a+d_2)(\xi+d_3+pZ_2)\\ &-Nd_3\xi[\xi+d_1+\beta(1-\varepsilon)V_2][(\xi-b+a+d_2)(1-f)(1-\varepsilon)\beta H_2+af(1-\varepsilon)\beta H_2]\\ &+Nd_3\xi(1-\varepsilon)\beta H_2[af(1-\varepsilon)\beta V_2+(\xi-b+a+d_2)(1-f)(1-\varepsilon)\beta V_2]\\ &+(\xi+d_4+mA_0)[\xi+d_1+\beta(1-\varepsilon)V_2](\xi-b+a+d_2)pcZ_2I_2\Big\}\\ &=0.\end{aligned} \tag{15}$$

It is clear that Eq. (15) has eigenvalue $\xi_1 = -d_5$. The remaining eigenvalues are determined by the following equation

$$\begin{aligned}&\xi(\xi+d_4+mA_0)[\xi+d_1+\beta(1-\varepsilon)V_2](\xi-b+a+d_2)(\xi+d_3+pZ_2)\\ &-Nd_3\xi[\xi+d_1+\beta(1-\varepsilon)V_2][(\xi-b+a+d_2)(1-f)(1-\varepsilon)\beta H_2+af(1-\varepsilon)\beta H_2]\\ &+Nd_3\xi(1-\varepsilon)\beta H_2[af(1-\varepsilon)\beta V_2+(\xi-b+a+d_2)(1-f)(1-\varepsilon)\beta V_2]\\ &+(\xi+d_4+mA_0)[\xi+d_1+\beta(1-\varepsilon)V_2](\xi-b+a+d_2)pcZ_2I_2\\ &=0.\end{aligned}$$

Using the steady state equalities $f(1-\varepsilon)\beta H_2V_2 + bL_2 = aL_2 + d_2L_2$, $(1-f)(1-\varepsilon)\beta H_2V_2 + aL_2 = d_3I_2 + pZ_2I_2$ and $Nd_3I_2 = d_4V_2 + mA_0V_2$, the above equation can be rewritten as

$$\xi^5 + b_1\xi^4 + b_2\xi^3 + b_3\xi^2 + b_4\xi + b_5 = 0,$$

where

$$\begin{aligned}b_1 &= d_4+mA_0+d_1+\beta(1-\varepsilon)V_2+a+d_2-b+d_3+pZ_2,\\ b_2 &= (d_3+pZ_2)(a+d_2-b)+(d_3+pZ_2)[d_1+\beta(1-\varepsilon)V_2]\\ &\quad +(a+d_2-b)[d_1+\beta(1-\varepsilon)V_2]\end{aligned}$$

$$
\begin{aligned}
&+(a+d_2-b)(d_4+mA_0)+(d_4+mA_0)[d_1+\beta(1-\varepsilon)V_2]\\
&+pcZ_2I_2+\frac{a(d_4+mA_0)L_2}{I_2},\\
b_3=&[d_1+\beta(1-\varepsilon)V_2](a+d_2-b)(d_3+pZ_2)\\
&+(d_4+mA_0)[d_1+\beta(1-\varepsilon)V_2](a+d_2-b)\\
&+Nd_3\beta^2(1-f)(1-\varepsilon)^2H_2V_2+(a+d_2-b)pcZ_2I_2\\
&+[d_1+\beta(1-\varepsilon)V_2]pcZ_2I_2\\
&+(d_4+mA_0)pcZ_2I_2+\frac{a(d_4+mA_0)[d_1+\beta(1-\varepsilon)V_2]L_2}{I_2},\\
b_4=&Nd_3a\beta^2f(1-\varepsilon)^2H_2V_2+(a+d_2-b)Nd_3\beta^2(1-f)(1-\varepsilon)^2H_2V_2\\
&+[d_1+\beta(1-\varepsilon)V_2](a+d_2-b)pcZ_2I_2+(d_4+mA_0)(a+d_2-b)pcZ_2I_2\\
&+(d_4+mA_0)[d_1+\beta(1-\varepsilon)V_2]pcZ_2I_2,\\
b_5=&(d_4+mA_0)[d_1+\beta(1-\varepsilon)V_2](a+d_2-b)pcZ_2I_2.
\end{aligned}
\tag{16}
$$

Since $\mathcal{R}_c>1$, we have $b_1,b_2,b_3,b_4,b_5>0$. From the first three equations in (16), it follows that

$$
\begin{aligned}
\acute{\triangle}_2=&b_1b_2-b_3\\
=&[d_4+mA_0+d_1+\beta(1-\varepsilon)V_2+a+d_2-b+d_3+pZ_2]\\
&\times\Big\{(d_3+pZ_2)(a+d_2-b)+(d_3+pZ_2)[d_1+\beta(1-\varepsilon)V_2]\\
&+(a+d_2-b)[d_1+\beta(1-\varepsilon)V_2]+(a+d_2-b)(d_4+mA_0)\\
&+(d_4+mA_0)[d_1+\beta(1-\varepsilon)V_2]+pcZ_2I_2+\frac{a(d_4+mA_0)L_2}{I_2}\Big\}\\
&-\Big\{[d_1+\beta(1-\varepsilon)V_2](a+d_2-b)(d_3+pZ_2)\\
&+(d_4+mA_0)[d_1+\beta(1-\varepsilon)V_2](a+d_2-b)+Nd_3\beta^2(1-f)(1-\varepsilon)^2H_2V_2\\
&+(a+d_2-b)pcZ_2I_2+[d_1+\beta(1-\varepsilon)V_2]pcZ_2I_2+(d_4+mA_0)pcZ_2I_2\\
&+\frac{a(d_4+mA_0)[d_1+\beta(1-\varepsilon)V_2]L_2}{I_2}\Big\}\\
=&(d_4+mA_0)\Big\{(d_3+pZ_2)(a+d_2-b)+d_1(d_3+pZ_2)\\
&+(a+d_2-b)(d_4+mA_0)+(d_4+mA_0)\\
&\times[d_1+\beta(1-\varepsilon)V_2]+\frac{a(d_4+mA_0)L_2}{I_2}\Big\}\\
&+[d_1+\beta(1-\varepsilon)V_2]\Big\{(d_3+pZ_2)[d_1+\beta(1-\varepsilon)V_2]\\
&+(a+d_2-b)[d_1+\beta(1-\varepsilon)V_2]+(a+d_2-b)(d_4+mA_0)
\end{aligned}
$$

$$
\begin{aligned}
&+(d_4+mA_0)[d_1+\beta(1-\varepsilon)V_2]\Big\}\\
&+(a+d_2-b)\Big\{(d_3+pZ_2)(a+d_2-b)+(d_3+pZ_2)[d_1+\beta(1-\varepsilon)V_2]\\
&+(a+d_2-b)[d_1+\beta(1-\varepsilon)V_2]+(a+d_2-b)(d_4+mA_0)\\
&+(d_4+mA_0)[d_1+\beta(1-\varepsilon)V_2]+\frac{a(d_4+mA_0)L_2}{I_2}\Big\}\\
&+(d_3+pZ_2)\Big\{(d_3+pZ_2)(a+d_2-b)+(d_3+pZ_2)[d_1+\beta(1-\varepsilon)V_2]\\
&+(a+d_2-b)[d_1+\beta(1-\varepsilon)V_2]+(a+d_2-b)(d_4+mA_0)\\
&+(d_4+mA_0)[d_1+\beta(1-\varepsilon)V_2]+pcZ_2I_2\\
&+\frac{a(d_4+mA_0)L_2}{I_2}\Big\}+\frac{a(d_4+mA_0)L_2}{I_2}\beta(1-\varepsilon)V_2\\
>&0,
\end{aligned}
\tag{17}
$$

where $(1-f)(1-\varepsilon)\beta H_2V_2+aL_2=d_3I_2+pZ_2I_2$ and $Nd_3I_2=d_4V_2+mA_0V_2$ have been used. Define

$$
\triangle_3^{'}=\begin{vmatrix} b_1 & 1 & 0\\ b_3 & b_2 & b_1\\ b_5 & b_4 & b_3\end{vmatrix}=b_3\triangle_2^{'}+b_1b_5-b_1^2b_4.
$$

From (16) and (17), we can obtain

$$
\begin{aligned}
b_3\triangle_2^{'}=&\Big\{[d_1+\beta(1-\varepsilon)V_2](a+d_2-b)(d_3+pZ_2)\\
&+(d_4+mA_0)[d_1+\beta(1-\varepsilon)V_2](a+d_2-b)\\
&+Nd_3\beta^2(1-f)(1-\varepsilon)^2H_2V_2+(a+d_2-b)pcZ_2I_2\\
&+[d_1+\beta(1-\varepsilon)V_2]pcZ_2I_2+(d_4+mA_0)pcZ_2I_2\\
&+\frac{a(d_4+mA_0)[d_1+\beta(1-\varepsilon)V_2]L_2}{I_2}\Big\}\Big\{(d_4+mA_0)\Big[(d_3+pZ_2)(a+d_2-b)\\
&+d_1(d_3+pZ_2)+(a+d_2-b)(d_4+mA_0)+(d_4+mA_0)[d_1+\beta(1-\varepsilon)V_2]\\
&+\frac{a(d_4+mA_0)L_2}{I_2}\Big]+[d_1+\beta(1-\varepsilon)V_2]\Big[(d_3+pZ_2)[d_1+\beta(1-\varepsilon)V_2]\\
&+(a+d_2-b)[d_1+\beta(1-\varepsilon)V_2]+(a+d_2-b)(d_4+mA_0)\\
&+(d_4+mA_0)[d_1+\beta(1-\varepsilon)V_2]\Big]+(a+d_2-b)\Big[(d_3+pZ_2)(a+d_2-b)\\
&+(d_3+pZ_2)[d_1+\beta(1-\varepsilon)V_2]+(a+d_2-b)[d_1+\beta(1-\varepsilon)V_2]\\
&+(a+d_2-b)(d_4+mA_0)+(d_4+mA_0)[d_1+\beta(1-\varepsilon)V_2]\\
&+\frac{a(d_4+mA_0)L_2}{I_2}\Big]+(d_3+pZ_2)\Big[(d_3+pZ_2)(a+d_2-b)
\end{aligned}
$$

$$
\begin{aligned}
&+ (d_3 + pZ_2)[d_1 + \beta(1-\varepsilon)V_2] + (a + d_2 - b)[d_1 + \beta(1-\varepsilon)V_2] \\
&+ (a + d_2 - b)(d_4 + mA_0) + (d_4 + mA_0)[d_1 + \beta(1-\varepsilon)V_2] + pcZ_2I_2 \\
&+ \frac{a(d_4 + mA_0)L_2}{I_2}\Bigg] + \frac{a(d_4 + mA_0)L_2}{I_2}\beta(1-\varepsilon)V_2\Bigg\},
\end{aligned}
$$

$$
\begin{aligned}
b_1b_5 =& \Big[d_4 + mA_0 + d_1 + \beta(1-\varepsilon)V_2 + a + d_2 - b + d_3 + pZ_2\Big] \\
&\times (d_4 + mA_0)[d_1 + \beta(1-\varepsilon)V_2](a + d_2 - b)pcZ_2I_2,
\end{aligned}
$$

and

$$
\begin{aligned}
b_1^2b_4 =& \Bigg\{(d_4 + mA_0)[d_4 + mA_0 + d_1 + \beta(1-\varepsilon)V_2 + a + d_2 - b + d_3 + pZ_2] \\
&+ [d_1 + \beta(1-\varepsilon)V_2][d_4 + mA_0 + d_1 + \beta(1-\varepsilon)V_2 + a + d_2 - b + d_3 + pZ_2] \\
&+ (a + d_2 - b)[d_4 + mA_0 + d_1 + \beta(1-\varepsilon)V_2 + a + d_2 - b + d_3 + pZ_2] \\
&+ (d_3 + pZ_2)[d_4 + mA_0 + d_1 + \beta(1-\varepsilon)V_2 + a + d_2 - b + d_3 + pZ_2]\Bigg\} \\
&\times \Bigg\{Nd_3a\beta^2f(1-\varepsilon)^2H_2V_2 + (a + d_2 - b)Nd_3\beta^2(1-f)(1-\varepsilon)^2H_2V_2 + [d_1 \\
&+ \beta(1-\varepsilon)V_2](a + d_2 - b)pcZ_2I_2 + (d_4 + mA_0)(a + d_2 - b)pcZ_2I_2 \\
&+ (d_4 + mA_0)[d_1 + \beta(1-\varepsilon)V_2]pcZ_2I_2\Bigg\}.
\end{aligned}
$$

After using the equalities $f(1-\varepsilon)\beta H_2V_2 + bL_2 = aL_2 + d_2L_2$, $(1-f)(1-\varepsilon)\beta H_2V_2 + aL_2 = d_3I_2 + pZ_2I_2$ and $Nd_3I_2 = d_4V_2 + mA_0V_2$, and rearranging terms, we derive

$$
\begin{aligned}
\acute{\triangle}_3 =& d_1(a + d_2 - b)(d_3 + pZ_2)\Bigg\{\acute{\triangle}_2 - \frac{a(d_4 + mA_0)L_2}{I_2}\beta(1-\varepsilon)V_2\Bigg\} \\
&+ \beta(1-\varepsilon)V_2(a + d_2 - b)(d_3 + pZ_2)\Bigg\{\acute{\triangle}_2 - (d_4 + mA_0)\Bigg[(d_3 + pZ_2) \\
&\times (a + d_2 - b) + (a + d_2 - b)(d_4 + mA_0) + \frac{a(d_4 + mA_0)L_2}{I_2}\Bigg] \\
&- [d_1 + \beta(1-\varepsilon)V_2](a + d_2 - b)(d_4 + mA_0) - (a + d_2 - b)^2(d_4 + mA_0) \\
&- (d_3 + pZ_2)\frac{a(d_4 + mA_0)L_2}{I_2} - \frac{a(a + d_2 - b)(d_4 + mA_0)L_2}{I_2}\Bigg\} \\
&+ d_1(d_4 + mA_0)(a + d_2 - b)\Bigg\{\acute{\triangle}_2 - (d_3 + pZ_2)pcZ_2I_2 \\
&- \frac{a(d_4 + mA_0)L_2}{I_2}\beta(1-\varepsilon)V_2\Bigg\} \\
&+ \beta(1-\varepsilon)V_2(a + d_2 - b)(d_4 + mA_0)\Bigg\{\acute{\triangle}_2 - \frac{a(d_4 + mA_0)^2L_2}{I_2}
\end{aligned}
$$

$$
\begin{aligned}
&- \frac{a(a+d_2-b)(d_4+mA_0)L_2}{I_2} - \frac{a(d_3+pZ_2)(d_4+mA_0)L_2}{I_2}\Bigg\} \\
&+ \frac{a(d_4+mA_0)[d_1+\beta(1-\varepsilon)V_2]L_2}{I_2}\Bigg\{\acute{\triangle}_2 - [d_1+\beta(1-\varepsilon)V_2](a+d_2-b) \\
&\times \beta(1-\varepsilon)V_2 - (a+d_2-b)^2\beta(1-\varepsilon)V_2 - (a+d_2-b) \\
&\times (d_4+mA_0)\beta(1-\varepsilon)V_2 - (d_3+pZ_2)(a+d_2-b)\beta(1-\varepsilon)V_2\Bigg\} \\
&+ Nd_3\beta^2(1-f)(1-\varepsilon)^2H_2V_2\Bigg\{(d_4+mA_0)\Bigg[d_1(d_3+pZ_2) \\
&+ (d_4+mA_0)[d_1+\beta(1-\varepsilon)V_2] + \frac{a(d_4+mA_0)L_2}{I_2}\Bigg] + [d_1+\beta(1-\varepsilon)V_2] \\
&\times \Bigg[(d_3+pZ_2)[d_1+\beta(1-\varepsilon)V_2] + (d_4+mA_0)[d_1+\beta(1-\varepsilon)V_2]\Bigg] \\
&+ (a+d_2-b)\frac{a(d_4+mA_0)L_2}{I_2} + (d_3+pZ_2)\Bigg[(d_3+pZ_2)[d_1+\beta(1-\varepsilon)V_2] \\
&+ (d_4+mA_0)[d_1+\beta(1-\varepsilon)V_2] + pcZ_2I_2 + \frac{a(d_4+mA_0)L_2}{I_2}\Bigg] \\
&+ \frac{a(d_4+mA_0)L_2}{I_2}\beta(1-\varepsilon)V_2\Bigg\} \\
&+ (a+d_2-b)pcZ_2I_2\Bigg\{(d_4+mA_0)\Bigg[d_1(d_3+pZ_2) + \frac{a(d_4+mA_0)L_2}{I_2}\Bigg] \\
&+ (a+d_2-b)\Bigg[(d_3+pZ_2)(a+d_2-b) + (d_3+pZ_2)[d_1+\beta(1-\varepsilon)V_2] \\
&+ \frac{a(d_4+mA_0)L_2}{I_2}\Bigg] \\
&+ (d_3+pZ_2)\Bigg[(d_3+pZ_2)(a+d_2-b) + (a+d_2-b)(d_4+mA_0) \\
&+ pcZ_2I_2 + \frac{a(d_4+mA_0)L_2}{I_2}\Bigg] + \frac{a(d_4+mA_0)L_2}{I_2}\beta(1-\varepsilon)V_2\Bigg\} \\
&+ [d_1+\beta(1-\varepsilon)V_2]pcZ_2I_2\Bigg\{(d_4+mA_0)\Bigg[d_1(d_3+pZ_2) + \frac{a(d_4+mA_0)L_2}{I_2}\Bigg] \\
&+ [d_1+\beta(1-\varepsilon)V_2]^2(d_3+pZ_2) + (a+d_2-b)\Bigg[(d_3+pZ_2)[d_1+\beta(1-\varepsilon)V_2] \\
&+ \frac{a(d_4+mA_0)L_2}{I_2}\Bigg] + (d_3+pZ_2)\Bigg[(d_3+pZ_2)(a+d_2-b) \\
&+ (d_3+pZ_2)[d_1+\beta(1-\varepsilon)V_2] + pcZ_2I_2 + \frac{a(d_4+mA_0)L_2}{I_2}\Bigg]
\end{aligned}
$$

$$+\frac{a(d_4+mA_0)L_2}{I_2}\beta(1-\varepsilon)V_2\Bigg\}+(d_4+mA_0)pcZ_2I_2\Bigg\{(d_4+mA_0)$$
$$\times\left[d_1(d_3+pZ_2)+\frac{a(d_4+mA_0)L_2}{I_2}\right]$$
$$+(a+d_2-b)\left[(d_4+mA_0)[d_1+\beta(1-\varepsilon)V_2]+\frac{a(d_4+mA_0)L_2}{I_2}\right]$$
$$+(d_3+pZ_2)\left[pcZ_2I_2+\frac{a(d_4+mA_0)L_2}{I_2}\right]+\frac{a(d_4+mA_0)L_2}{I_2}\beta(1-\varepsilon)V_2\Bigg\}.$$

In the above equation, we subtract some terms from $\acute{\triangle}_2$ to simplify the form. However, it follows from (17) that these terms are all positive. This means that $\acute{\triangle}_3 > 0$. Moreover,

$$\acute{\triangle}_4=\begin{vmatrix} b_1 & 1 & 0 & 0\\ b_3 & b_2 & b_1 & 1\\ b_5 & b_4 & b_3 & b_2\\ 0 & 0 & b_5 & b_4\end{vmatrix}=b_4\acute{\triangle}_3-b_2b_5\acute{\triangle}_2+b_1b_4b_5-b_5^2,$$

By applying a similar approach, we can show that $\acute{\triangle}_4 > 0$. From this, we obtain $\acute{\triangle}_5 = b_5\acute{\triangle}_4 > 0$. By the Routh-Hurwitz criterion, we show that all roots of (15) have negative real parts. Hence, the infected equilibrium with CTL immune response E_2 is locally asymptotically stable when $\mathcal{R}_c > 1$.

REFERENCES

[1] J. Ananworanich, B. McSteen and M. L. Robb, Broadly neutralizing antibody and the HIV reservoir in acute HIV infection: A strategy toward HIV remission?, *Curr. Opin. HIV AIDS*, **10** (2015), 198-206.

[2] C. Armbruster, G. M. Stiegler, B. A. Vcelar, et al., A phase I trial with two human monoclonal antibodies (hMAb 2F5, 2G12) against HIV-1, *AIDS Lond. Engl.*, **16** (2002), 227-233.

[3] M. Asokan, J. Dias, C. Liu, et al., Fc-mediated effector function contributes to the in vivo antiviral effect of an HIV neutralizing antibody, *Proc. Natl. Acad. Sci. USA*, **117** (2020), 18754-18763.

[4] A. Badamchi-Zadeh, L. J. Tartaglia, P. Abbink, et al., Therapeutic efficacy of vectored PGT121 gene delivery in HIV-1-infected humanized mice, *J Virol.*, **92** (2018), e01925-17.

[5] A. B. Balazs, J. Chen, C. M. Hong, et al., Antibody-based protection against HIV infection by vectored immunoprophylaxis, *Nature*, **481** (2012), 81-84.

[6] S. Belmonti, S. Di Giambenedett and F. Lombardi, Quantification of total HIV DNA as a marker to measure viral reservoir: Methods and potential implications for clinical practice, *Diagnostics*, **12** (2022), 39.

[7] T. Bruel, F. Guivel-Benhassine, S. Amraoui, et al., Elimination of HIV-1-infected cells by broadly neutralizing antibodies, *Nat. Commun.*, **7** (2016), 10844.

[8] J. Carrillo, B. Clotet and J. Blanco, Antibodies and antibody derivatives: New partners in HIV eradication strategies, *Front. Immunol.*, **9** (2018), 2429.

[9] M. Chazal, P. Nzounza, C. Pique, et al., Loss of infectivity of HIV-1 particles produced by mobile lymphocytes, *PLoS One*, **9** (2014), e109601.

[10] J. M. Conway and A. S. Perelson, Post-treatment control of HIV infection, *Proc. Natl. Acad. Sci. USA*, **112** (2015), 5467-5472.

[11] Q. Deng, T. Guo, Z. Qiu, et al., Towards a new combination therapy with vectored immunoprophylaxis for HIV: Modeling "shock and kill" strategy, *Math. Biosci.*, **355** (2023), 108954.

[12] R. Desikan, R. Raja and N. M. Dixit, Early exposure to broadly neutralizing antibodies may trigger a dynamical switch from progressive disease to lasting control of SHIV infection, *PLoS Comput. Biol.*, **16** (2020), e1008064.

[13] D. J. DiLillo and J. V. Ravetch, Differential Fc-receptor engagement drives an anti-tumor vaccinal effect, *Cell*, **161** (2015), 1035-1045.
[14] C. Gaebler, L. Nogueira, E. Stoffel, et al., Prolonged viral suppression with anti-HIV-1 antibody therapy, *Nature*, **606** (2022), 368-374.
[15] J. D. Gunst, M. H. Pahus, M. Rosás-Umbert, et al., Early intervention with 3BNC117 and romidepsin at antiretroviral treatment initiation in people with HIV-1: A phase 1b/2a, randomized trial, *Nat. Med.*, **28** (2022), 2424-2435.
[16] T. Guo and Z. Qiu, The effects of CTL immune response on HIV infection model with potent therapy, latently infected cells and cell-to-cell viral transmission, *Math. Biosci. Eng.*, **16** (2019), 6822-6841.
[17] T. Guo, Z. Qiu, K. Kitagawa, et al., Modeling HIV multiple infection, *J. Theor. Biol.*, **509** (2021), 110502.
[18] T. Guo, Z. Qiu and L. Rong, Analysis of an HIV model with immune responses and cell-to-cell transmission, *Bull. Malays. Math. Sci. Soc.*, **43** (2020), 581-607.
[19] A. Halper-Stromberg, C.-L. Lu, F. Klein, et al., Broadly neutralizing antibodies and viral inducers decrease rebound from HIV-1 latent reservoirs in humanized mice, *Cell*, **158** (2014), 989-999.
[20] HIV-CAUSAL Collaboration, M. Ray, R. Logan, et al., The effect of combined antiretroviral therapy on the overall mortality of HIV-infected individuals, *AIDS*, **24** (2010), 123-137.
[21] Y. C. Ho, L. Shan, N. N. Hosmane, et al., Replication-competent noninduced proviruses in the latent reservoir increase barrier to HIV-1 cure, *Cell*, **155** (2013), 540-551.
[22] I. V. Kholodenko, D. V. Kalinovsky, E. V. Svirshchevskaya, et al., Multimerization through pegylation improves pharmacokinetic properties of scFv fragments of GD2-specific antibodies, *Molecules*, **24** (2019), 3835.
[23] Y. Liu, W. Cao, M. Sun, et al., Broadly neutralizing antibodies for HIV-1: Efficacies, challenges and opportunities, *Emerg. Microbes Infect.*, **9** (2020), 194-206.
[24] C.-L. Lu, D. K. Murakowski, S. Bournazos, et al., Enhanced clearance of HIV-1-infected cells by broadly neutralizing antibodies against HIV-1 in vivo, *Science*, **352** (2016), 1001-1004.
[25] L. L. Lu, T. J. Suscovich, S. M. Fortune, et al., Beyond binding: Antibody effector functions in infectious diseases, *Nat. Rev. Immunol.*, **18** (2018), 46-61.
[26] G. Maartens, C. Celum and S. R. Lewin, HIV infection: Epidemiology, pathogenesis, treatment, and prevention, *Lancet*, **384** (2014), 258-271.
[27] B. C. Mackness, J. A. Jaworski, E. Boudanova, et al., Antibody Fc engineering for enhanced neonatal Fc receptor binding and prolonged circulation half-life, *MAbs*, **11** (2019), 1276-1288.
[28] M. Malbec, F. Porrot, R. Rua, et al., Broadly neutralizing antibodies that inhibit HIV-1 cell to cell transmission, *J. Exp. Med.*, **210** (2013), 2813-2821.
[29] N. Martin, S. Welsch, C. Jolly, et al., Virological synapsemediated spread of human immunodeficiency virus type 1 between T cells is sensitive to entry inhibition, *J. Virol.*, **84** (2010), 3516-3527.
[30] S. Mester, M. Evers, S. Meyer, et al., Extended plasma half-life of albumin-binding domain fused human IgA upon pH-dependent albumin engagement of human FcRn in vitro and in vivo, *MAbs*, **13** (2021), 1893888.
[31] D. C. Montefiori, Measuring HIV neutralization in a luciferase reporter gene assay, *Methods Mol. Biol.*, **485** (2009), 395-405.
[32] J. Niessl, A. E. Baxter, P. Mendoza, et al., Combination anti-HIV-1 antibody therapy is associated with increased virus-specific T cell immunity, *Nat. Med.*, **26** (2020), 222-227.
[33] Y. Nishimura, O. K. Donau, J. Dias, et al., Immunotherapy during the acute SHIV infection of macaques confers long-term suppression of viremia, *J. Exp. Med.*, **218** (2021), e20201214.
[34] Y. Nishimura, R. Gautam, T. W. Chun, et al., Early antibody therapy can induce long-lasting immunity to SHIV, *Nature*, **543** (2017), 559-563.
[35] L. Reh, C. Magnus, M. Schanz, et al., Capacity of broadly neutralizing antibodies to inhibit HIV-1 cell-cell transmission is strain- and epitope-dependent, *PLoS Pathog.*, **11** (2015), e1004966.
[36] L. Rong and A. S. Perelson, Asymmetric division of activated latently infected cells may explain the decay kinetics of the HIV-1 latent reservoir and intermittent viral blips, *Math. Biosci.*, **217** (2009), 77-87.
[37] L. Rong and A. S. Perelson, Modeling HIV persistence, the latent reservoir, and viral blips, *J. Theor. Biol.*, **260** (2009), 308-331.

[38] M. Rosás-Umbert, J. D. Gunst, M. H. Pahus, et al., Administration of broadly neutralizing anti-HIV-1 antibodies at ART initiation maintains long-term CD8+ T cell immunity, *Nat. Commun.*, **13** (2022), 6473.
[39] K. O. Saunders, Conceptual approaches to modulating antibody effector functions and circulation half-life, *Front. Immunol.*, **10** (2019), 1296.
[40] P. Schommers, H. Gruell, M. E. Abernathy, et al., Restriction of HIV-1 escape by a highly broad and potent neutralizing antibody, *Cell*, **180** (2020), 471-489. e22.
[41] A. I. Schriek, Y. L. T. Aldon, M. J. van Gils, et al., Next-generation bNAbs for HIV-1 cure strategies, *Antiviral Res.*, **222** (2024), 105788.
[42] J. D. Siliciano, J. Kajdas, D. Finzi, et al., Long-term follow-up studies confirm the stability of the latent reservoir for HIV-1 in resting CD4+ T cells, *Nat Med.*, **9** (2003), 727-728.
[43] G. Stiegler, C. Armbruster, B. Vcelar, et al., Antiviral activity of the neutralizing antibodies 2F5 and 2G12 in asymptomatic HIV-1-infected humans: A phase I evaluation, *AIDS Lond. Engl.*, **16** (2002), 2019-2025.
[44] H. R. Thieme, Convergence results and a Poincaré-Bendixson trichotomy for asymptotically autonomous differential equations, *Journal of Mathematical Biology*, **30** (1992), 755-763.
[45] T. Tiller, E. Meffre, S. Yurasov, et al., Efficient generation of monoclonal antibodies from single human B cells by single cell RT-PCR and expression vector cloning, *J. Immunol. Methods.*, **329** (2008), 112-124.
[46] X. Wang, G. Mink, D. Lin, et al., Influence of raltegravir intensification on viral load and 2-LTR dynamics in HIV patients on suppressive antiretroviral therapy, *J. Theor. Biol.*, **416** (2017), 16-27.
[47] *WHO*, HIV/AIDS: Fact sheet, 2023. Available from: `http://www.who.int/mediacentre/factsheets/fs360/en/`.
[48] C. Yan and W. Wang, Modeling HIV dynamics under combination therapy with inducers and antibodies, *Bull. Math. Biol.*, **81** (2019), 2625-2648.
[49] Y. Yang, Y. Xiao and J. Wu, Pulse HIV vaccination: Feasibility for virus eradication and optimal vaccination schedule, *Bull. Math. Biol.*, **75** (2013), 725-751.
[50] W. Zhang and L. A. Ellingson, Detecting and resetting tipping points to create more HIV post-treatment controllers with bifurcation and sensitivity analysis, *SIAM Journal on Applied Mathematics*, **84** (2024), S493-S514.

Received May 2024; revised August 2024; early access August 2024.